1 **Planktonic foraminifera assemblage composition and flux dynamics inferred from an annual**
2 **sediment trap record in the Central Mediterranean Sea**

4 Thibauld M. Béjard[1*], Andrés S. Rigual-Hernández[1], Javier Pérez Tarruella[1], José-Abel Flores[1], Anna
5 Sanchez-Vidal[2], Irene Llamas-Cano[2], Francisco J. Sierro[1]

7 1. Área de Paleontología, Departamento de Geología, Universidad de Salamanca, Salamanca, Spain
8 2. GRC Geociències Marines, Departament de Dinàmica de la Terra i de l'Oceà, Universitat de
9 Barcelona, Spain

11 *** Correspondence:** Thibauld M. Béjard (thibauld.bejard@usal.es)

13 **Keywords:** sediment trap - Sicily Channel - Mediterranean Sea - planktonic foraminifera - seasonal
14 variations - environmental change

16 Changes suggested by reviewer #1
17 Changes suggested by reviewer #2
18 Changes suggested by reviewers #1 and #2
19 Changes added by the authors
20
21 **Abstract**

23 The Sicily Channel, located in the Central Mediterranean Sea, represents a key point for the regional
24 oceanographic circulation as it is considered the sill that separates the western and eastern basins.
25 Therefore, it is considered a unique zone regarding the well-documented west-to-east
26 Mediterranean productivity gradient. Here we present a time series of settling planktonic
27 foraminifera assemblages from November 2013 to October 2014. 19 samples from the sediment
28 trap C01 deployed at a water depth of around 400 m have been used. More than 3700 individuals
29 and 15 different species have been identified. *Globorotalia inflata*, *Globorotalia truncatulinoides*,
30 *Globigerina bulloides*, *Globigerinoides ruber* and *ruber* (pink) were the five main species identified,
31 accounting for more than 85% of the total foraminifera.
32 The total planktonic foraminifera flux mean value was 630 shells m^{-2} d^{-1}, with a minimum value of
33 45 shells m^{-2} d^{-1} displayed during late autumn 2013 and a maximum of 1890 shells m^{-2} d^{-1} reached
34 during spring 2014. This is likely due to the regional oceanographic configuration and the marked
35 seasonality in the surface circulation. During spring and winter, the Atlantic waters dominate the
36 surface circulation, bringing cool and nutrient enriched waters. This results in a planktonic
37 foraminifera flux increase and a dominance of western basin taxa. During summer and autumn, the
38 circulation is dominated by the eastern warm and oligotrophic Levantine water, which leads to a
39 planktonic foraminifera flux decrease and the dominance of easter basin species. Our comparison
40 with satellite derived SST and chlorophyll-*a* data showed that *G. inflata* was associated with cool
41 and nutrient rich conditions, while both *G. ruber* morphotypes were associated with warm and
42 oligotrophic conditions. However, no trends were identified for *G. truncatulinoides* or *G. bulloides*.

43 As the latter species flux increased coincidently with that of benthic foraminifera one, we considered
44 that this species might have a resuspended origin.
45 The comparison of the Sicily Channel data with other Mediterranean time series located in the
46 Alboran Sea, Gulf of Lions and the Levantine basin was carried out. Our data indicates that the
47 annualized planktonic foraminifera flux was lower than in the westernmost Alboran Sea but higher
48 than in the easternmost Levantine basin. However, The Sicily Channel species diversity was the
49 highest among the compared zones, highlighting the influence of the different basins and its
50 transitional aspect from a planktonic foraminifera population perspective.
51 Finally, we compared the settling planktonic foraminifera assemblage with the assemblages from
52 seabed sediment located in the vicinity of the Sicily Channel. The differences with the seabed
53 populations varied according to the sites studied. The deep-dwelling species dominated the settling
54 assemblages samples, while eutrophic and oligotrophic species were significantly more abundant in
55 the sediment. Finally, a high-resolution chronology comparison allowed to show that this planktonic
56 foraminifera population shift likely developed during the late Holocene prior to the industrial period,
57 however, its causes remain uncertain.
58
59 **1. Introduction**
60
61 Planktonic foraminifera are a group of marine calcareous single-celled protozoans with a
62 cosmopolitan distribution. Around 50 morphospecies of planktonic foraminifera have been
63 described in today's oceans (Schiebel and Hemleben, 2017), and although most of those species are
64 surface dwellers, some species can be found in waters below 2000 m (Schiebel and Hemleben,
65 2005). Their abundance and distribution are affected by a wide array of factors, such as
66 temperature, salinity, chlorophyll-a and nutrient concentrations, among others (Hemleben et al.,
67 1989; Schiebel and Hemleben, 2005). According to Schiebel, (2002), the production and export of
68 their calcareous shells account for 23 to 56% of the open marine $CaCO_3$ flux, thereby playing a key
69 role in the marine carbon cycle. Moreover, the high preservation potential of their shells makes
70 them one of the most used groups for multi-proxy studies. Numerous paleoclimatic (e.g. Barker and
71 Elderfield, 2002; Lirer et al., 2014; Margaritelli et al., 2020; Sierro et al., 2005) and
72 paleoceanographic (Cisneros et al., 2016; Ducassou et al., 2018; Margaritelli et al., 2022; Toucanne
73 et al., 2007) reconstructions have used planktonic foraminifera as a proxy. In addition, their capacity
74 to reflect the water column's chemical properties has propelled studies that have focused on the
75 impact of recent climate and environmental variability on the water column in different parts of the
76 ocean (e.g. Azibeiro et al., 2023; Beer et al., 2010; Bijma et al., 2002; Chapman, 2010; Marshall et
77 al., 2013; Osborne et al., 2016). As marine calcifying organisms, they are considered particularly
78 vulnerable to the ongoing ocean warming and acidification (Bijma et al., 2002; Fox et al., 2020). Shell
79 calcification of several foraminifera species has been showed to decrease in response to ocean
80 acidification, and therefore, changes in the weight of their shells are considered an indicator of the
81 ocean acidification impact on different timescales (Béjard et al., 2023; de Moel et al., 2009; Fox et
82 al., 2020; Kroeker et al., 2013; Moy et al., 2009; Pallacks et al., 2023). In contrast, ocean warming
83 has been proposed to produce an opposite effect on foraminifera calcification, as some studies have

84   documented that an increase in water temperature results in larger shells and enhanced growth
85   rates (Lombard et al., 2011, 2009; Schmidt et al., 2006).

86   Despite the wide array of studies focused on planktonic foraminifera ecology and distribution,
87   several aspects of their ecology remain uncertain, such as their ecological tolerance limits (Mallo et
88   al., 2017), their geographical and temporal distributions and contribution to the marine
89   biogeochemical cycles (Jonkers and Kučera, 2015). As major contributors to the pelagic calcite
90   production (Schiebel, 2002), understanding their life cycle on different time scales is essential for
91   constraining the role they play in the marine carbon cycle and the impact of environmental change
92   on these organisms. In this regard, sediment traps represent a powerful tool to improve our
93   knowledge of planktonic foraminifera ecology and their impact on the biogeochemical cycles, as
94   they allow the monitoring of foraminifera shell fluxes for extended periods, thereby allowing to
95   document their seasonal and interannual variability and estimate their contribution to annual
96   budgets of carbonate export to the seafloor (Jonkers et al., 2019).

97   The Mediterranean Sea is a semi-enclosed sea often considered a "miniature ocean" (Bethoux et
98   al., 1999) from an oceanographic point of view or a "laboratory basin" (Bergamasco and Malanotte-
99   Rizzoli, 2010) for studying processes occurring on a global scale. In addition, it is supersaturated
100   regarding calcite (Álvarez et al., 2014), a key aspect in foraminifera studies, as this parameter favors
101   shell preservation and represents one of the main environmental controls on planktonic
102   foraminifera abundance and calcification (Aldridge et al., 2012; Marshall et al., 2013; Osborne et al.,
103   2016). These features make it an interesting zone of the global ocean to study the life cycle and
104   seasonal response to changing environmental conditions of calcifying plankton. The Sicily Channel,
105   in the central Mediterranean, is the sill that divides the Mediterranean into its western and eastern
106   basins. It is a choke point for the regional surface and deep-water circulation (Malanotte-Rizzoli et
107   al., 2014; Pinardi et al., 2015) and a transition region regarding the well-known west-to-east
108   oligotrophy gradient, functioning as a "biological corridor" (Siokou-Frangou et al., 2010) known in
109   the Mediterranean (Navarro et al., 2017).

110   Despite these characteristics, time series that focused on planktonic foraminifera in the
111   Mediterranean Sea are scarce. So far, the best monitored regions are the Alboran Sea (Bárcena et
112   al., 2004; Hernández-Almeida et al., 2011), the Gulf of Lions (Rigual-Hernández et al., 2012), and
113   more recently, the Levantine Basin (Avnaim-Katav et al., 2020). The latter studies showed that
114   planktonic foraminifera followed a unimodal distribution with maximum shell export occurring
115   during the months of April-May, February-March and February respectively, which agreed with the
116   local hydrographic conditions. However, the central Mediterranean remains understudied and
117   poorly documented regarding both continuous time series and planktonic foraminifera dynamics.

118   Therefore, this work aims to provide new planktonic foraminifera data from a sediment trap
119   mooring line located in the Channel of Sicily to improve the current knowledge about their
120   community composition and seasonal patterns in the central Mediterranean. For that purpose, here
121   we document the magnitude and composition of planktonic foraminifera fluxes identified in the
122   >150 μm fraction (i.e. the most commonly used size fraction for studying planktonic foraminifera
123   distribution) from November 2013 to October 2014. We compare our planktonic foraminifera data
124   with a suite of environmental parameters to assess the main environmental drivers that control the
125   seasonal variations in the composition and abundance of the sinking planktonic foraminifera

126   assemblages. To provide further insight on a regional and global scale of the planktonic foraminifera
127   association and fluxes identified here, we compare our data with other time series from the
128   Mediterranean, Atlantic Ocean and other regions of the world's oceans. Lastly, we compared the
129   assemblages collected by the sediment with seabed sediment located in the vicinity of the Sicily
130   Channel to document the potential shift in recent planktonic foraminifera populations.

2. Study area

The Mediterranean is an elongated, semi-enclosed sea with an anti-estuarine circulation. It is considered to be a concentration basin (Bethoux et al., 1999) in which the evaporation exceeds the freshwater inputs, forcing a negative hydrological balance (Robinson and Golnaraghi, 1994). This negative balance is compensated by the entrance of surface oceanic water from the Atlantic Ocean through the Channel of Gibraltar. The colder and nutrient richer Atlantic Waters (AW) spread eastward into the Mediterranean basin (Millot, 1991; Pinardi et al., 2015), where they progressively become warmer, saltier and more oligotrophic as they mix with resident waters (Modified Atlantic Waters – MAW. Also known as Atlantic Waters – AW). MAW circulate following a cyclonic circuit along the Algerian coast (Algerian Current – AC) (Malanotte-Rizzoli et al., 2014; Millot, 1999) and divide into two main branches at the entrance of the Sicily Channel (Figure 1a). One of these branches spreads into the northwestern part of the basin, into the Tyrrhenian Sea, where it continues its path cyclonically. The second branch flows south of Sicily into the Ionian Sea (Lermusiaux and Robinson, 2001). In the Sicily channel itself, the water masses are split again in two different streams (Béranger et al., 2004): (i) the Atlantic Tunisian Current (ATC) that flows to the southeast following the African coast; and (ii) the Atlantic Ionian Stream (AIS) that flows into the deep eastern part of the basin (Figure 1b) and contributes to the MAW transport in the eastern Mediterranean (Jouini et al., 2016; Lermusiaux and Robinson, 2001).

The Sicily Channel is located in the central Mediterranean (Figure 1a) and acts as a sill that topographically separates the western and eastern Mediterranean basins. The circulation through the Sicily Channel is characterized by water masses that flow in opposite directions at different depths of the water column (Béranger et al., 2004; Garcia-Solsona et al., 2020; Pinardi et al., 2015; Schroeder et al., 2017). The Levantine Intermediate Water (LIW), which enters the Channel from the Ionian Sea, occupies the deeper part of the water column along with occasional thin Eastern Mediterranean Deep Water layers (Gasparini et al., 2005; Lermusiaux and Robinson, 2001). The Ionian Water (IW) can be present at intermediate depths (Figure 1), while the MAW cover the surface to subsurface part of the water column (Garcia-Solsona et al., 2020; Warn-Varnas et al., 1999). Temperature and salinity range from 15-17 °C and 37.2-37.8 psu for the MAW, 15-16.5 °C and 37.8-38.4 psu for the IW and 13.7-13.9°C and 38.7-38.8 psu for the LIW (Astraldi et al., 2002; Bouzinac et al., 1999; Robinson et al., 1999). Lastly, it is important to note, that the surface circulation in the Sicily Channel presents a large seasonal variability concerning the water masses distribution (Béranger et al., 2004; Lermusiaux and Robinson, 2001). Surface circulation experiences a substantial seasonality in the Sicily Channel: during late autumn to late spring, the MAW dominate the surface circulation, allowing nutrient and chlorophyll-enriched waters to enter the Channel (Astraldi et al., 2002; D'Ortenzio, 2009). In turn, summer and autumn are dominated by LIW waters. Deep-water circulation remains relatively stable on a seasonal scale (Béranger et al., 2004) with a continuous LIW presence over the year. Finally, during summer, an upwelling settles in the Sicily Channel, allowing the impoverished LIW to reach the surface (Lermusiaux and Robinson, 2001).

Regarding its nutrient distributions, the Mediterranean Sea is generally considered an oligotrophic to ultraoligotrophic sea (Krom et al., 1991). However, this oligotrophy is not homogenous and displays a clear west-to-east gradient which is reflected in the nutrient concentration and algal

biomass accumulation derived from colour remote sensing (Navarro et al., 2017; Siokou-Frangou et al., 2010). The eastern part of the Mediterranean is considered to be more nutrient depleted than the western part of the basin (Krom et al., 2005; Raimbault et al., 1999), with N:P ratios around 50:1 (Krom et al., 2005). At times of maximum annual algal concentration, primary productivity (PP) in the Levantine Basin reaches values of ca. 0.1 g C m^{-2}d^{-1} (Hazan et al., 2018). This value is substantially lower than those recorded in the high productivity regions of the western basin such as the Gulf of Lions, ca. 0.4-0.65 g C m^{-2}d^{-1} (Gaudy et al., 2003; Rigual-Hernández et al., 2012), or the Alboran Sea, ca. 0.3-1.3 g C m^{-2}d^{-1} (Bárcena et al., 2004; Morán and Estrada, 2001) during the corresponding period.
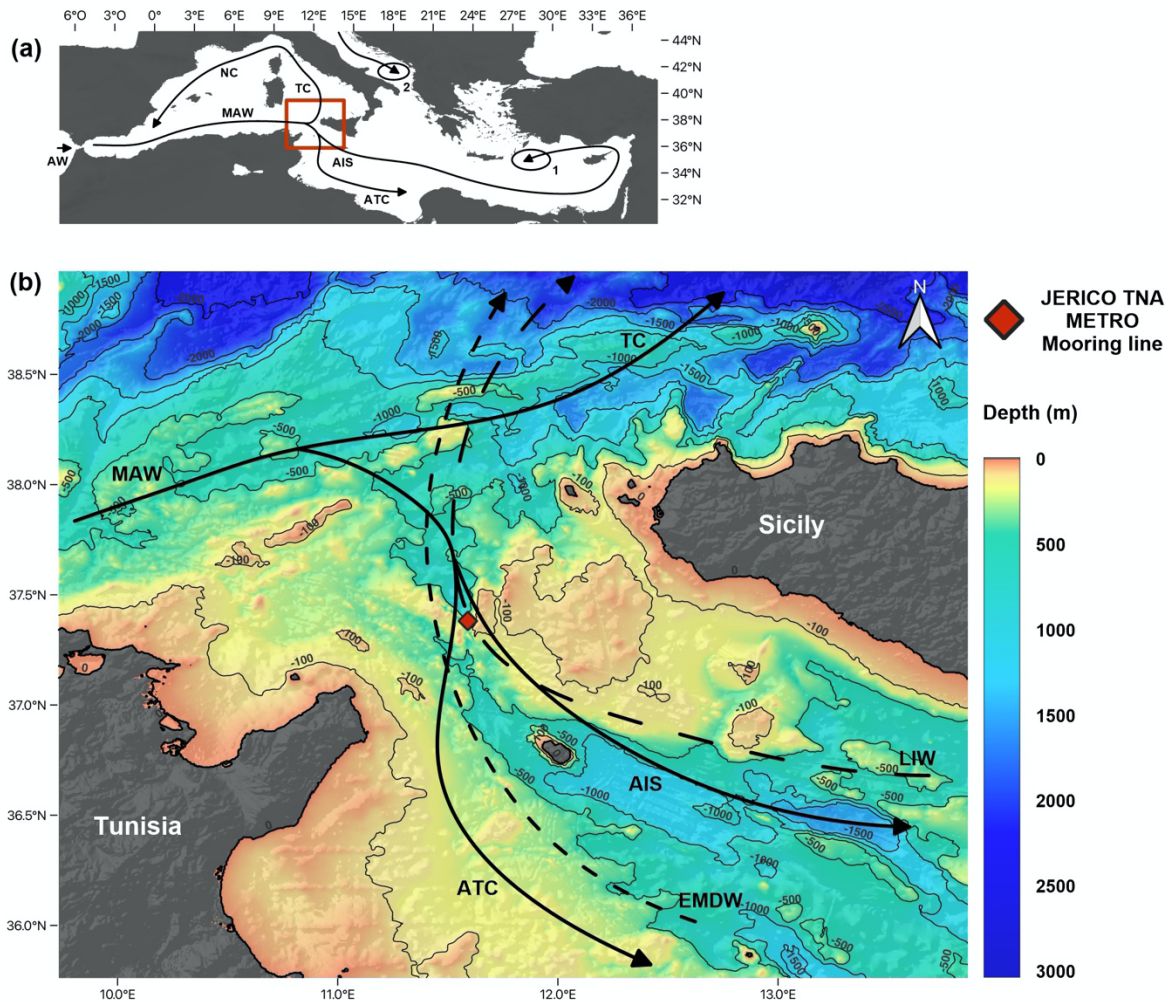
Figure 1. (a) Mediterranean Sea general surface circulation (Astraldi et al., 2002; Béranger et al., 2004; Incarbona et al., 2011; Macias et al., 2019) and location of the study zone. The ellipses show the deep-water formation zones for the LIW (1) and the EMDW (2). **(b)** Regional oceanographic and geographic setting of the Sicily Channel. The red diamond represents the location of the JERICO TNA METRO C01 mooring line. Black continuous lines represent the surface circulation dominated by the Atlantic Ionian Stream (AIS) and the Atlantic Tunisian Current (ATC); while dashed lines show deep-water circulation influences by the Levantine Intermediate Water (LIW) and the Eastern Mediterranean Deep Water (EMDW). The difference in the dashed lines period stands for the occasional aspect of the EMDW. The topographic model was downloaded from the GEBCO database.

192

3. Material and methods

193

3.1. Field experiments

The sediment trap (Figure 1) was deployed in the C01 mooring line maintained by ISMAR-CNR in the Sicily Channel (37.38°N, 11.59°E) thanks to a TransNational Access (TNA) call in the FP7 JERICO project (Mediterranean sediment Trap Observatory). The mooring line was equipped with a sequential sampling sediment trap located 413 m below the sea surface in a water column of around 450 m deep. The sediment trap was a PPS3/3 model, conical in shape with a 2.5 height/diameter ratio and equipped with 12 sampling cups. Further information about this sediment trap configuration and model can be found in Heussner et al., (2006, 1990).

Here we present data from November 2013 to mid-October 2014. The sampling period was 15 to 16 days from November 2013 to July 2014 and from September 2014 to October 2014. Between July 2014 and September 2014, the sampling was set to 31 days. Before deployment and to limit the degradation of the material caught, sediment trap sampling cups from both mooring lines were filled with a 5% formalin solution prepared with 40% formaldehyde mixed with 0.45 μm filtered seawater. The solution was then buffered with sodium borate to keep the pH stable and prevent the dissolution of carbonate.

3.2 Processing of sediment trap samples

After the recovery, the cups were stored at 2-4°C until their processing according to the procedure of Heussner et al., (1990). In the laboratory, the largest swimmers that entered the trap were removed by wet sieving through a 1 mm nylon and samples were subsequently split into 6 aliquots using a peristaltic pump. One sub-sample was used for total mass flux measurements, after having <1mm swimmers and formaldehyde removed.

Another subsample of a total of 19 samples from the sediment trap were processed for micropaleontological analyses in the micropaleontology laboratory of the Geology department at the University of Salamanca. The samples consisted of aliquots of 1/6 of the original mooring line cups and were preserved in seawater, with a pH between 7.6 and 7.8. All samples were first wet sieved to separate the <63μm fraction and then dry sieved to separate the 63-150 and >150 μm fractions. The washing was carried out with a potassium phosphate-buffered solution (pH= 7.5) to prevent carbonate dissolution.

3.3 Planktonic foraminifera identification, flux calculations and imaging

The planktonic foraminifera identification (Plate 1) and counting to the species level were carried out in the >150 μm fraction using a microscope (Leica Wild M3B). To have a representative picture of the planktonic foraminifera population, the complete samples were analyzed (i.e. no splits were applied). Identification was carried out according to Schiebel and Hemleben, (2017). A total of 15 species were identified (Plate 1): *Globigerinella siphonifera*, *G. calida*, *Globigerinoides sacculifer*, *G. ruber*, *G. ruber* (pink), *Globoturborotalita tenella*, *G. rubescens*, *Orbulina universa*, *Globorotalia truncatulinoides*, *G. inflata*, *G. scitula*, *Globigerina bulloides*, *G. falconensis*, *Neogloboquadrina*

incompta and *Turborotalita quinqueloba* (Plate 1). In addition, benthic foraminifera shells were identified to the lowest taxonomic level possible and counted. The 150 μm size limit was used to compare our results with other time series and seabed sediment populations as it is widely used in planktonic foraminifera studies, however, we acknowledge that some "small-sized" species such as *N. incompta* and *G. tenella* may be undersampled as their adult size tends to be smaller (Chernihovsky et al., 2023).

The foraminifera fluxes were calculated according to the following formula:

$$PF \ (shells \ m^{-2} \ d^{-1}) = \frac{(N \ x \ aliq.) \ x \ SD^{-1}}{0.1256}$$

"PF" stands for planktonic foraminifera, "N" accounts for the number of individuals identified, "aliq." refers to the aliquot (1/6 for all samples) and "SD" represents the sampling interval that the sediment trap cup stayed open. Relative abundance for each species was also calculated for all samples.

Here we refer to the planktonic foraminifera collected by the sediment trap as the settling assemblage.

Lastly, to describe the seasonal flux variations and to put our results into a regional context and be coherent with previous studies, each season was defined as spring (March–May), summer (June–August), autumn (September–November) and winter (December–February).

To showcase the species collected by the traps (Plate 1), foraminifera imaging was carried out using a Nikon SMZ18 stereomicroscope equipped with a Nikon DS-Fi3 camera and the image processing software NISElements (version 5.11.03).

3.4. Satellite-derived environmental parameters

To assess the possible relationship of planktonic foraminifera fluxes with environmental variability, ~~key environmental parameters, namely~~ satellite-derived chlorophyll-*a* and Sea Surface Temperatures (SSTs) were retrieved from global data sets. Satellite-derived chlorophyll-*a* concentration (mg m^{-3}) was obtained from MODIS L3m satellite through NASA's Giovanni web interface with an 8-day and 4 km resolution for a 0.2 x 0.2° area around the mooring location between 01/10/2013 to 01/11/2014. Additionally, sea surface temperature SST (°C) were also obtained from the same site with the same resolution to use as a proxy for water temperature and water column stratification.

3.5 Planktonic foraminifera flux and surface sediment data from other Mediterranean settings

In order to put into context our observations with the regional variability of planktonic foraminifera communities in the Mediterranean Sea, modern planktonic foraminifera flux datasets were retrieved from different sites. Foraminifera fluxes of: (i) the Levantine basin (LevBas) were obtained from Avnaim-Katav et al., (2020); (ii) the Gulf of Lions (stations Planier - PLA, and Lacaze Duthiers - LCD) from Rigual-Hernández et al., (2012); (iii) and the Alboran Sea (stations ALB 1F and ALB 5F) from both Bárcena et al., (2004) and Hernández-Almeida et al., (2011). The foraminifera fluxes of the Gulf of Lions and Alboran Sea concerned the >150 μm fraction, while the ones from the Levantine basin represented the >125 μm fraction (Figure 7).

274   Core-top data from the ForCenS database (Siccha and Kucera, 2017) was used to compare the
275   planktonic foraminifera abundance patterns from the C01 mooring line with the seabed sediment.
276   Only seabed sediment located on a 2.5 degree difference in both latitude and longitude was selected
277   to compare our data with sites in the vicinity of the Sicily Channel. This corresponded to a total of
278   16 core-tops part of the MARGO database. The complete details of the latter can be found in the
279   Supplementary data.
280   Additionally, the planktonic foraminifera population data from two box-cores analyzed by Incarbona
281   et al., (2019) were also included: sites 342 (36.42°N, 13.55°E) and 407 (36.23°N, 14.27°E). These two
282   sites are located in the Sicily Channel and they provide a robust chronology (^{210}Pb) that allowed to
283   document abundance changes across the recent Holocene. The dating covered the years 1558 to
284   1994 CE. Here we compared the sediment trap from the C01 mooring line samples with the mean
285   relative abundance from the 23 (site 342) and 24 (site 407) samples available.
286   Finally, to have a more complete picture of the modern planktonic foraminifera communities
287   currently living the surface ocean, the annual integrated data of our sediment trap was compared
288   with the BONGO nets data from Mallo et al., (2017), specifically, with the sample retrieved in the
289   axis of the Sicily Channel (37.08°N, 13.18°E) in Spring 2013.
290

291   **3.6 Statistical analysis**
292   To have uninterrupted monthly and daily values from NASA's Giovanni environmental parameters
293   that coincide with the mean sampling date from the sediment trap, a daily resampling has been
294   carried out using QAnalySeries software.
295   Pearson correlation and *p*-value tests between the foraminifera abundances and the environmental
296   parameters (SST and chlorophyll-*a*) were carried out with the Past4 program. A *p* < 0.05 was used
297   to denote statistical significance.
298   In addition, a canonical correspondence analysis (CCA) was also used to evaluate the influence of
299   both SST and chlorophyll-*a* on foraminifera species fluxes. A CCA is a correspondence analysis of a
300   species matrix where each site has given values for one or more environmental variables (SST and
301   chlorophyll-*a* concentration in this case). The ordination axes are linear combinations of the
302   environmental variables. A CCA is considered an example of direct gradient analysis, where the
303   gradient in environmental variables is known and the species abundances/fluxes are considered to
304   be a response or to be affected by this gradient (Nielsen, 2000).
305   Additionally, to evaluate the magnitude of the foraminifera fluxes across major regions of the
306   Mediterranean, an estimation of the annual planktonic foraminifera flux (shells m^{-2} y^{-1}) was
307   calculated using the sediment trap data from the literature review and our study. To that purpose,
308   the data was annualized according to the following formula:

$$Annual\ PFF = \sum(PF\ x\ SD + cPF\ x\ mSD)$$

310   Where "PFF" stands for planktonic foraminifera flux (shells m^{-2} d^{-1}), "SD" accounts for sampling days,
311   "cPF" represents calculated planktonic foraminifera flux (shells m^{-2} d^{-1}) and "mSD" stands for missing
312   sampling days. "cPF" calculation depended on the site. For the datasets retrieved from the Sicily
313   Channel and the Levantine basin, less than 20 sampling days were missing, so the corresponding
314   planktonic foraminifera fluxes were replaced by the mean of the first and last flux values recorded.
315   The two datasets from the Alboran Sea displayed more than 70 missing days, so the corresponding

316   flux values used were a mean of the two closest months to the missing data. Concerning the two
317   time series from the Gulf of Lions, they covered more than one year. Therefore, a mean year was
318   estimated: a mean monthly flux value was calculated for all 12 months based on all the available
319   measurements and then multiplied by the corresponding mean duration of each month, and then,
320   all monthly fluxes were added together.
321   To compare the species richness and diversity across the previously described sites, Simpson (D) and
322   Shannon/Weiner (H/W) indexes were calculated. Here, we reported the inverse Simpson index (1-
323   D). None of these indexes were calculated for the Alboran Sea sites (ALB 1F and ALB 5F) because
324   only information about the four main species was documented (Bárcena et al., 2004; Hernández-
325   Almeida et al., 2011).
326   Finally, the squared chord distance (SCD) between the C01 sediment trap and every core top sample
327   downloaded from the ForCenS database (Siccha and Kucera, 2017) planktonic foraminifera relative
328   abundance was calculated. It is a widely used metric in palaeoecological and paleontological studies
329   as it is the most effective index for identifying the closest analogues in planktonic foraminifera
330   datasets (Prell, 1985). This is mainly because it shows the best balance in weighing the contribution
331   of abundant and rare species in a given association (Jonkers et al., 2019). In this study, SCD values
332   lower than 0.25 have been considered as reliable analogues (Ortiz and Mix, 1997).
333
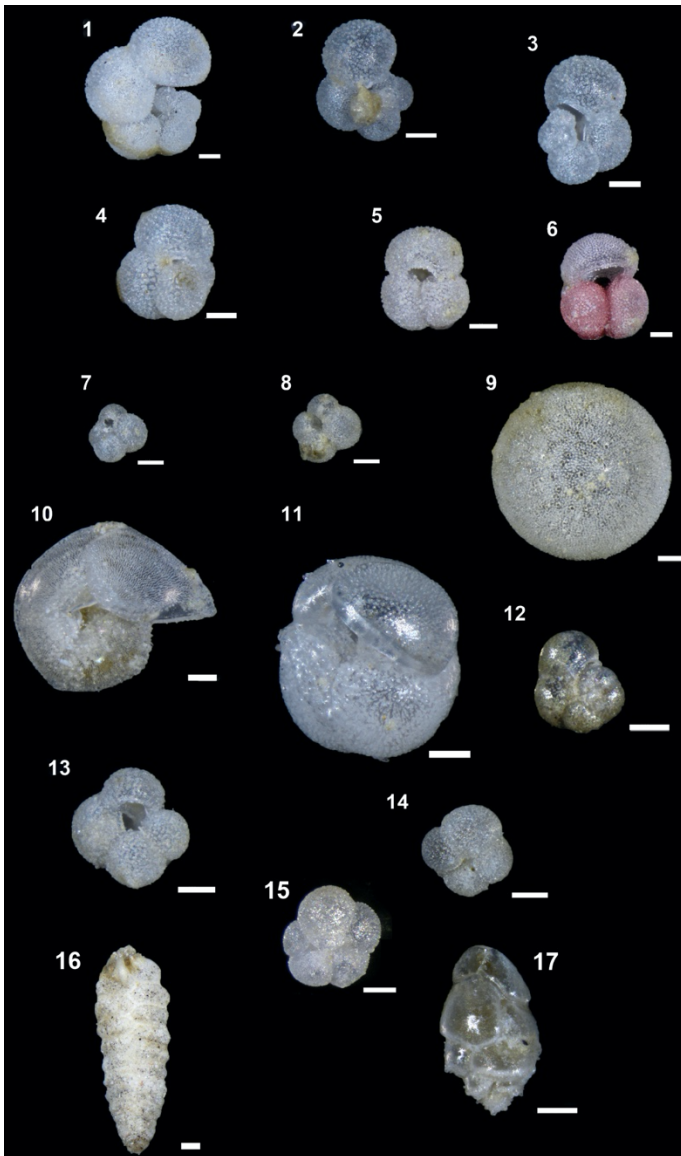
334
335 **Plate 1.** Planktonic **(1-15)** and the most common benthic foraminifera **(16-17)** species trapped in the
336 sediment trap in mooring line C01. The white scale bars on all figures represent 100 μm. **(1)** *G.*
337 *siphonifera,* side view. **(2)** *G. calida*, umbilical view. **(3)** *G. calida*, apertural view. (**4**) *G. sacculifer*,
338 umbilical view. (**5**) *G. ruber*, umbilical view. **(6)** *G. ruber* (pink), umbilical view. **(7)** *G. tenella*, umbilical
339 view. **(8)** *G. rubescens*, umbilical view. **(9)** *O. universa*. **(10)** *G. truncatulinoides*, umbilical view. **(11)**. *G.*
340 *inflata*, apertural view. **(12)** *G. scitula*, umbilical view. **(13)** *G. bulloides*, umbilical view. **(14)** *N. incompta*,
341 umbilical view. **(15).** *T. quinqueloba,* umbilical view. **(16)** *Textularia spp.* **(17)** *Bulimina marginata*,
342 apertural view.

343
344 **4. Results**

345
346 **4.1 General considerations of the planktonic foraminifera assemblages**

347

348 **Table 1.** Counts and key statistics of the planktonic foraminifera species and the benthic foraminifera
349 group from the > 150 μm fraction identified in the 19 sediment trap cups of the C01 mooring line. Mean,
350 maximum (Max), minimum (Min), standard deviation (SD) of the relative abundance and fluxes. Raw
351 counts also include a total and % of the total description. Note that *G. falconensis* was documented but
352 not included in the table due to its scarcity (only one individual was identified).

	G. sipho.	G. cal.	G. sacc.	G. rub.	G. rub.(p.)	G. ten.	G. rubesc.	O. univ.	G. truncat.	G. inf.	G. sci.	G. bull.	N. inc.	T. quin.	Benthics	Total planktonic
COUNTS (N)																
Mean	2.5	3.1	4.1	6.5	5.2	1.1	3.7	3.9	37.0	109.2	1.3	16.2	1.5	0.5	7.4	195.9
Max	6	11	10	22	40	5	9	15	118	456	7	111	8	3	42	633
Min	0	0	0	1	0	0	0	0	1	1	0	0	0	0	1	14
SD	1.8	2.8	3.2	5.6	9.2	1.5	2.5	4.1	33.2	132.5	2.3	26.4	2.3	1.1	9.2	
Total	48	59	78	124	99	21	71	74	703	2075	24	307	29	10	141	3723
% of total	1.3	1.6	2.1	3.3	2.7	0.6	1.9	2.0	18.9	55.7	0.6	8.2	0.8	0.3	3.3	
ABUNDANCES (%)																
Mean	2.0	2.7	2.8	5.5	5.7	0.9	4.0	3.0	20.5	41.6	1.9	7.3	1.8	0.2	5.2	
Max	7.4	10.2	8.1	16.0	32.5	8.5	14.3	16.9	46.1	72.0	8.8	26.7	21.4	1.7	12.5	
Min	0.0	0.0	0.0	0.5	0.0	0.0	0.0	0.0	7.1	1.6	0.0	0.0	0.0	0.0	0.6	
SD	2.0	2.7	2.4	4.7	10.1	1.9	4.3	3.9	9.0	24.0	3.2	6.5	4.8	0.4	3.9	
FLUXES (shells m^{-2} d^{-1})																
Mean	7.9	10.2	13.2	19.6	15.8	3.6	12.0	11.0	113.8	354.9	3.3	57.2	5.3	1.8	24.8	629.8
Max	26.1	47.8	34.7	65.7	127.4	21.7	28.7	35.0	368.5	1361.5	22.3	482.0	34.7	13.0	182.4	1889.9
Min	0.0	0.0	0.0	3.2	0.0	0.0	0.0	0.0	3.2	3.2	0.0	0.0	0.0	0.0	3.0	44.6
SD	6.5	11.1	11.3	17.7	29.6	5.8	8.6	10.7	107.2	426.4	6.3	110.7	8.8	3.9	39.9	

354 A total of 3723 planktonic foraminifera shells and 141 benthic foraminifera were counted.
355 Planktonic foraminifera were identified at the species level, resulting in a total of 15 different species
356 identified (Plate 1). A mean of 196 planktonic foraminifera specimens per sample were identified,
357 with a minimum of 14 individuals in November 2013 and a maximum of 633 individuals in mid-
358 March 2014 (Table 1).
359 According to the raw counts results, the most abundant species was *G. inflata*, which represented
360 55.7% of the total planktonic foraminifera individuals. The second most represented species was *G.*
361 *truncatulinoides*, with 18.9%, followed by *G. bulloides* with 8.2%. These three species alone
362 accounted for more than 80% of the planktonic foraminifera identified. The remaining species
363 abundances were below 5%. *G. ruber*, *G. ruber* (pink), *O. universa*, *G. rubescens* and *G. sacculifer*
364 represented between 2 and 3.3 % of the total individuals. Species like *G. tenella*, *G. scitula*, *N.*
365 *incompta* and *T. quinqueloba* were very scarce and accounted individually for less than 1% of the
366 total planktonic individuals (Table 1). Finally, only one individual of *G. falconensis* has been
367 identified. Note that *G. inflata*, *G. truncatulinoides* and *G. ruber* were the only species present in all
368 samples. Concerning the differentiation between lobulated and sac-type *Globigerinoides*, we mainly
369 found individuals belonging to the first group, the sac-type individuals were scarce. The latter were
370 identified mainly during summer and autumn.

 Finally, the benthic foraminifera only represented 3.3% of the total foraminifera identified and 80%
372 of the individuals were identified in the two samples retrieved during April 2014 (see Supplementary
373 data).
374

375 **4.2 Total mass and planktonic foraminifera fluxes**
376
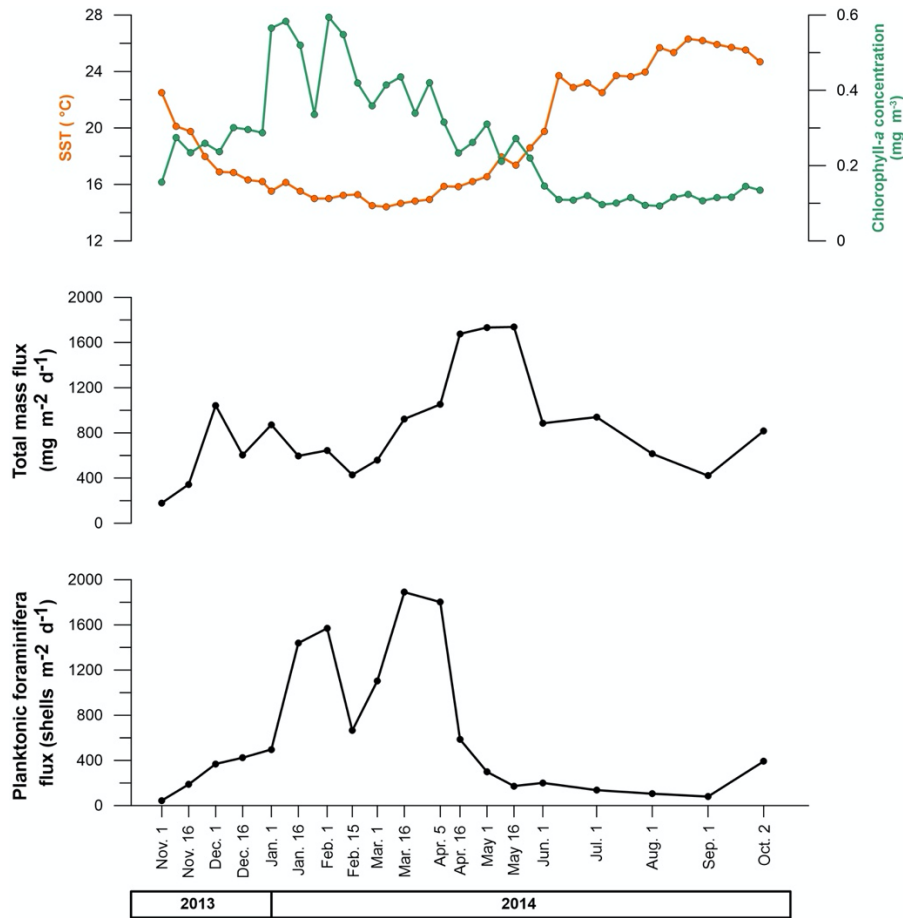
377
378 **Figure 2.** Total mass flux (TMF) (mg m^{-2} day^{-1}), total planktonic foraminifera flux (PFF) (shells m^{-2} day^{-1}),
379 SST (°C) and chlorophyll-*a* concentration (mg m^{-3}) changes between November 2013 and October 2014.
380

381 The mean total mass flux for the whole period of the study was 772.5 mg m^{-2} d^{-1}, with a maximum
382 value of 1737.7 mg m^{-2} d^{-1} and a minimum value of 179.5 mg m^{-2} d^{-1} reached in mid-May 2014 and
383 November 2013 respectively (Figure 2). Higher total mass flux values were reached during spring
384 2014, while lower values appeared during both autumn 2013 and 2014.
385 Planktonic foraminifera mean flux across the interval studied was 629.8 shells m^{-2} d^{-1} with a
386 maximum value of 1889.9 shells m^{-2} d^{-1} and a minimum of 44.6 shells m^{-2} d^{-1} reached in mid-March
387 2014 and in November 2013 respectively. Higher values occurred during two periods, early spring
388 and winter 2014, while the lower ones occurred from late spring to fall 2014. Overall, the seasonal
389 mean values were 1194.3 shells m^{-2} d^{-1} for the winter period, 612.3 shells m^{-2} d^{-1} for spring, 283.5
390 shells m^{-2} d^{-1} for autumn and finally 107.2 shells m^{-2} d^{-1} for summer.

391   SST mean value was 19.2 °C and values ranged between a maximum of 26.1 and a minimum of 14.5
392   °C. The mean chlorophyll-a value was 0.27 mg m^{-3}, the maximum value displayed was 0.56 mg m^{-3}
393   while the minimum one was 0.09 mg m^{-3} (Figure 2).
394

4.3 Foraminifera species fluxes

396   Overall, most of the planktonic foraminifera species collected by the trap exhibited either a uni-
397   modal or bi-modal flux distribution with a few exceptions (Figure 3).
398   *Globorotalia inflata* exhibited the highest fluxes of all species, with a mean flux of 368 shells m^{-2} d^{-1}
399   throughout the record, with peak values in mid-March 2014 (1361 shells m^{-2} d^{-1}) and minimum in
400   November 2013 (3 shells m^{-2} d^{-1}). *G. truncatulinoides* was the second most important contributor
401   (mean of 114 shells m^{-2} d^{-1}), with a maximum in mid-February and a minimum in November 2013
402   (368 and 3 shells m^{-2} d^{-1}, respectively). *G. bulloides* was the third most important contributor to the
403   total planktonic foraminifera fluxes with a mean flux of 57.2 shells m^{-2} d^{-1} and maximum values
404   registered in April 2014 and minima in November 2013 (482 and 0 shells m^{-2}d^{-1}, respectively).
405   The remaining species displayed mean fluxes lower than 50 shells m^{-2} d^{-1}. *G. calida*, *G. ruber*, *G. ruber*
406   (pink), *G. rubescens* and *O. universa* mean fluxes were comprised between 10 and 20. Among these
407   species, *G. ruber* and *G. ruber* (pink) stood out and showed maximum fluxes of 66 shells m^{-2} d^{-1} in
408   February 2014 and 127 shells m^{-2} d^{-1} in October 2014, respectively. The remaining species, *G.*
409   *siphonifera*, *G. scitula*, ~~*G. falconensis,*~~ *N. incompta* and *T. quinqueloba* mean and maximum fluxes
410   were lower than 10 and 35 shells m^{-2} d^{-1}, respectively, thereby representing a low contribution to
411   the total foraminifera fluxes.
412   Finally, it is worth noting that benthic foraminifera were also collected by the trap, displaying a mean
413   flux of 25 shells m^{-2} d^{-1}. The peak contribution of these taxa was recorded in April 2014 (182 shells
414   m^{-2} d^{-1}), and a minimum value in January 2014 (3 shells m^{-2} d^{-1}). In terms of annualized foraminifera
415   flux, their contribution was only a 1.1% of the total foraminifera identified of which 75% was
416   recorded during April 2014 (Figure 6).
417
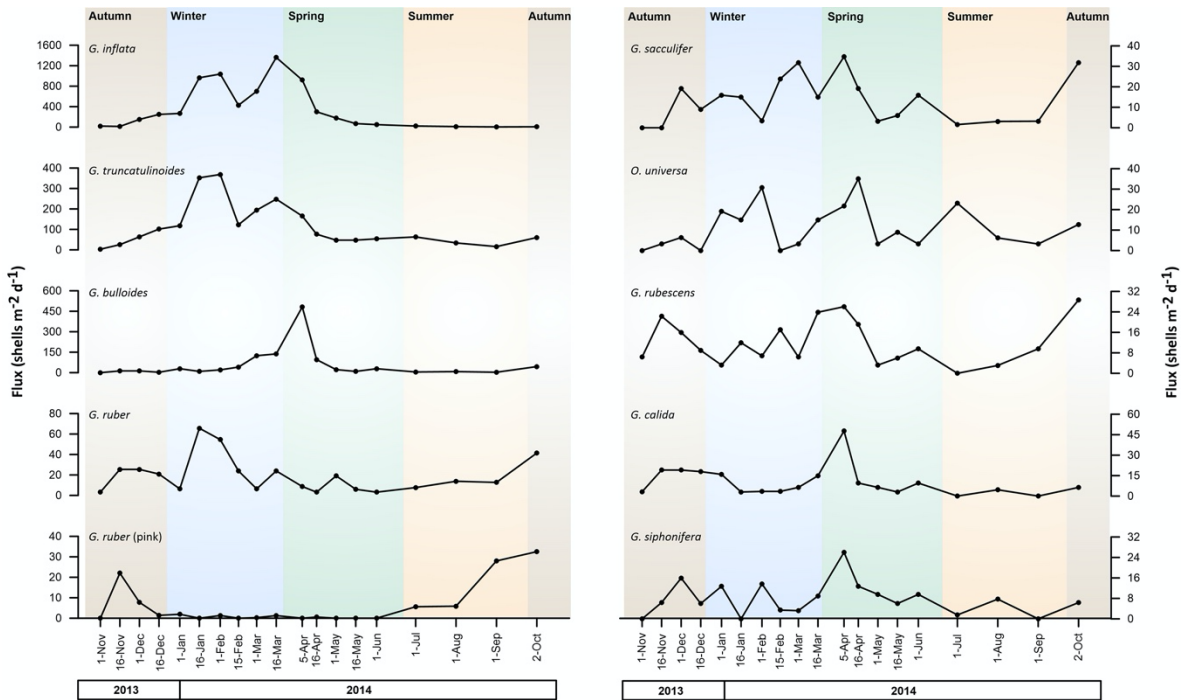
Figure 3. Planktonic foraminifera fluxes (shells m⁻² d⁻¹) and relative abundances (%, grey lines) from November 2013 to October 2014 of the 10 most abundant species identified. Note that the scale of the fluxes and abundances depend on the species. Background colour filling represents the different seasons: brown for autumn, blue for winter, green for spring and orange for summer.

The variations in relative abundance differed according to the species. Most of the species displayed a unimodal distribution across the studied interval (Supplementary Figure 3), with some exceptions such as *G. siphonifera*, *G. calida* or *G. ruber*. Overall, *G. inflata* dominated the association from late autumn until mid-spring. Its relative abundance was comprised between 72% reached in mid-March 2014 and around 2% in mid-November 2013 (Figure 3). *G. truncatulinoides* relative abundance pattern was similar to that of *G. inflata*, with maximum values in autumn and late summer. The lowest relative abundance was reached in November 2013: around 7%, while the highest abundance was 46% in July 2014. Note that despite the seasonality of its abundance, the amplitude of its relative abundance change was low compared to other species (Figure 3). In turn, the third most abundant foraminifera species, *G. bulloides*, displayed a pronounced seasonal change in its relative abundance reaching values up to 27% in early spring (April 2014) and dropping to about 5-8% in November 2014.

Secondary contributors, such as *G. siphonifera* and *G. sacculifer* reached their maximum contributions (~8%) in August and June 2014, respectively, *G. calida* in mid-November 2013 (10%), *G. ruber* in November 2013 (16%), *G. ruber* pink in October 2014 (32.5%) and both *G. rubescens* and *O. universa* exhibited their maximum contributions (with 14-15% for both species) in November 2013 and in July 2014, respectively.

Overall, *G. inflata* is the only species that displayed its maximum mean relative abundance during winter: 64%. *G. siphonifera*, *G. sacculifer*, and *G. bulloides*, maximum mean relative abundances were reached during spring: 3%, 3.5%, 14% respectively. *G. calida*, *G. tenella*, *G. rubescens* and *N.*

444   *incompta* maximum mean abundances appeared to be in autumn: 5.7%, 2.2%, 8% and 4.8%
445   respectively. Finally, *G. ruber*, *G. ruber* (pink), *O. universa*, *G. truncatulinoides* and *G. scitula*
446   maximum mean relative abundances were displayed in summer: 11.6%, 13.2%, 8.9%, 32.8% and
447   6.4% respectively (Supplementary Figure 3).
448

449   **4.4 Chlorophyll-*a* and SST impact on foraminifera fluxes**
450
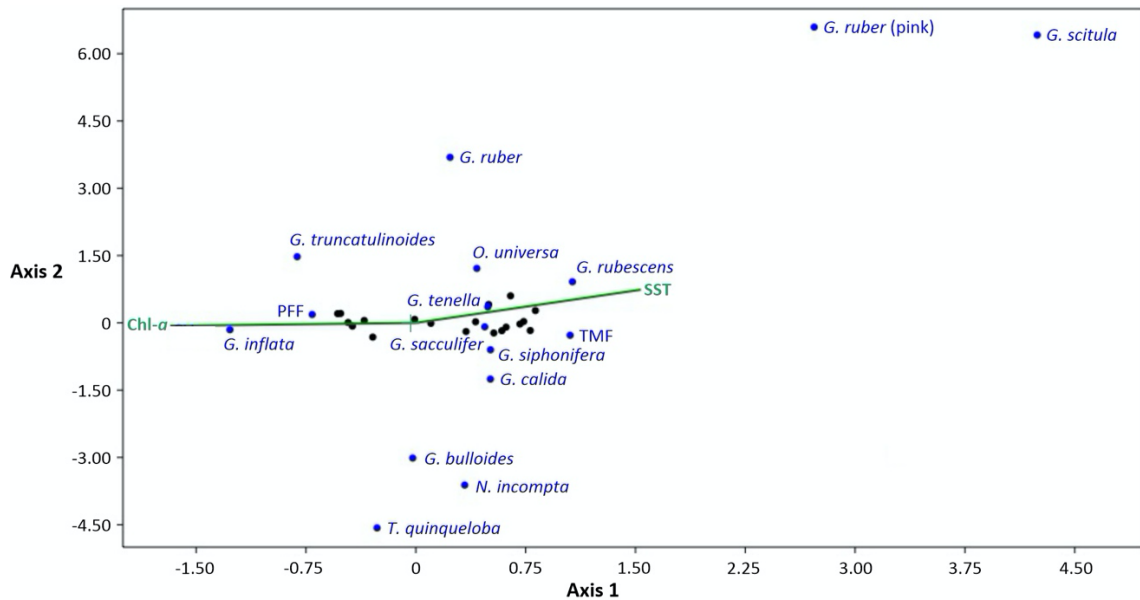
451
452   **Figure 4.** CCA analysis of all the planktonic foraminifera species flux with the SST (°C) and the chlorophyll-
453   *a* ("chl-*a*" in the CCA, in mg m^{-3}) as the explanatory variables. The total mass flux ("TMF") and planktonic
454   foraminifera flux ("PFF") are also included. Black dots represent the 19 sediment trap samples studied.
455

456   A CCA (see section 3.4) was carried out to characterize the impact of both the SST and the
457   chlorophyll-*a* on the planktonic foraminifera fluxes (Figure 4).
458   Axis 1 shows, overall, the differences between deep and surface dwellers. Total planktonic
459   foraminifera flux (PFF) and the fluxes of *G. inflata* and *G. truncatulinoides* are positively affected by
460   the chlorophyll-*a* concentration and negatively affected by the SST. On the other hand, *G. ruber*, *G.*
461   *ruber* (pink) and *G. scitula* fluxes showed an opposite pattern, being positively related with the SST
462   and negatively with the chlorophyll-*a* concentration. *O. universa*, *G. rubescens*, *G. tenella*, *G.*
463   *sacculifer, G. siphonifera* and *G. calida* fluxes are positively correlated with the SST and negatively
464   with chlorophyll-*a* concentration, nonetheless, the impact of these parameters is weaker compared
465   with the previous species. Finally, *G. bulloides*, *N. incompta* and *T. quinqueloba* fluxes are slightly
466   positively influenced by the chlorophyll-*a* concentration, however. Axis 2 tends to separate the
467   species between the different trophic regimes. Overall, it confirms that, in the one hand, *G. ruber*,
468   *G. ruber* (pink) and *G. scitula* display a strong negative correlation with chlorophyll-*a* and therefore
469   an affinity for oligotrophic and warm conditions; and on the other hand, shows that *G. bulloides*, *N.*
470   *incompta* and *T. quinqueloba* display a positive correlation with chlorophyll-*a* and eutrophic

473

5. Discussion

475

5.1 Seasonal variations in the magnitude of planktonic foraminifera fluxes in the Sicily Channel

477

478 The strong seasonality in the planktonic foraminifera fluxes registered by the trap is generally similar

479 in amplitude to previous studies in the Mediterranean (Bárcena et al., 2004; Rigual-Hernández et

480 al., 2012) and other temperate settings (Kuroyanagi and Kawahata, 2004; Wilke et al., 2009),

481 thereby suggesting the C01 record mainly reflects the temporal variations in planktonic foraminifera

482 abundance in the upper water column. Therefore, next, we discuss the influence of oceanographic

483 controls on the planktonic foraminifera fluxes.

484 Our data shows that, despite differences in the magnitude of their fluxes, most of the species

485 identified display their maximum flux during winter, winter/spring transition or spring (Figure 3)

486 thereby coinciding with the period of maximum algal biomass accumulation and coldest SSTs (Figure

487 2). The enhanced primary productivity during winter and spring is mostly related to an

488 intensification of the chlorophyll-*a* and nutrient richer MAW flow into the Eastern Mediterranean

489 basin (D'Ortenzio, 2009; Pinardi et al., 2015; Siokou-Frangou et al., 2010). Our CCA results (Figure 4)

490 show that, although the flux patterns increase during winter and spring, only the planktonic

491 foraminifera flux, *G. inflata*, *G. truncatulinoides* and arguably *G. bulloides* (further discussed below)

492 fluxes are negatively related to SSTs and positively with the chlorophyll-*a* concentration. The

493 dominance of the planktonic foraminifera fluxes by these three species and their affinity for

494 mesotrophic waters is not surprising as *G. inflata* and *G. truncatulinoides* are typically associated

495 with the MAW, winter water mixing events and hydrologic fronts in the western Mediterranean,

496 while *G. bulloides* is generally associated with eutrophic environments linked to upwelling

497 conditions (Azibeiro et al., 2023). Overall, these three taxa have been described to be dominant

498 during winter in various western regions of the Mediterranean, such as the Alboran Sea (Bárcena et

499 al., 2004; Hernández-Almeida et al., 2011), the Provençal basin and in the Gulf of Lions (Pujol and

500 Grazzini, 1995; Rigual-Hernández et al., 2012). Interestingly *G. inflata*, *G. truncatulinoides* and *G.*

501 *bulloides* are almost absent in the eastern part of the basin, most likely due to the low algal biomass

502 accumulation (Avnaim-Katav et al., 2020; Thunell, 1978).

503 Conversely, species such as *G. ruber*, *G. ruber* (pink), *G. scitula*, *G. rubescens* and *G. sacculifer* display

504 their maximum fluxes in summer or autumn (Figure 3). During the warm periods, summer and

505 autumn, the eastward advection of Atlantic waters in the Sicily Channel is weakened due to an

506 increased meandering of the ATC (Figure 1) and the local hydrography patterns (Béranger et al.,

507 2004), leading to a local water column stratification period which is also well documented in the

508 whole Mediterranean basin during summer (Siokou-Frangou et al., 2010). This translates into a

509 reduced MAW influence, and a larger influence of the LIW at intermediate depths (Astraldi et al.,

510 2002, 2001; Jouini et al., 2016). Therefore, the water column becomes warmer, saltier and more

511 nutrient depleted than the general conditions of the western basin (Gasparini et al., 2005; Navarro

512 et al., 2017; Siokou-Frangou et al., 2010) and provides the necessary environmental and

oceanographical configuration for eastern basins taxa to develop or being transported from the easternmost part of the Mediterranean. Indeed, our CCA results (Figure 4) support these observations (Figure 3). The latter species have been described to reach their maximum abundances in the eastern part of the Mediterranean, specifically in the Ionian and Levantine basins during both summer and autumn (Avnaim-Katav et al., 2020; Pujol and Grazzini, 1995).

Some species, such as *O. universa* or *G. calida*, do not display a clear flux pattern over the period studied. CCA results suggest that these species have an affinity for warm and less productive conditions. These taxa are considered widespread in the Mediterranean basin, although their relative contributions are generally higher in the eastern part of the basin (Avnaim-Katav et al., 2020; Pujol and Grazzini, 1995; Thunell, 1978). Lastly, it is important to note that the low number of specimens of *G. falconensis*, *N. incompta*, *T. quinqueloba* and *G. tenella* found in our samples, makes the estimation of shell fluxes for these species unreliable. These results are not surprising, since *N. incompta* is mainly found in the northwestern part of the basin owing to cold and eutrophic conditions (Azibeiro et al., 2023; Millot and Taupier-Letage, 2005) while *T. quinqueloba* has generally been associated to cool Atlantic waters or cool marginal seas (Azibeiro et al., 2023).

In summary, planktonic foraminifera flux was maximum during winter and spring, coinciding with the maximum seasonal eastward advection that brings MAW further east into the Sicily Channel. These waters are less saline and nutrient enriched compared to the easternmost waters from the Levantine basin. *G. inflata*, *G. truncatulinoides* and *G. bulloides* (the three most abundant species that dominate the PFF), which are species described to come from the western basins, are probably brought by the MAW and then dominate the planktonic foraminifera population. On the other hand, during summer and autumn, the eastward advection weakens, allowing the LIW and AIS to dominate the surface circulation due to the water column stratification and set favourable conditions for eastern basin dominant taxa such as both morphotypes of *G. ruber*, *G. rubescens*, *G. sacculifer*. This results in a significantly decreased planktonic foraminifera flux due to the absence of western basin dominant species.

5.2 Species succession, ecology and impact of the SST and chlorophyll-*a*

The time series of settling planktonic foraminifera reflects a diverse assemblage with species with contrastingly different ecological preferences, encompassing a wide range of depth habitats and diverse feeding strategies. Overall, the annual assemblage composition agrees well with previous ship-board observations (Pujol and Grazzini, 1995) in the Channel of Sicily during VICOMED 1988 cruise, where *G. inflata*, *G. truncatulinoides* and *G. bulloides* were documented as the most abundant taxa.

Next, we discuss the ecology of the most abundant species and the impact of chlorophyll-*a* and SST on their distribution. We also discuss the foraminifera groups suggested by Jonkers and Kučera, (2015), to explore their correlation with the previous parameters on an interannual scale. The latter work proposed 3 groups: group 1 is formed by tropical and subtropical species, group 2 consists of temperate to subpolar taxa, and group 3 represents the deep-dwelling species. These groups were described as a result of the seasonal maximum fluxes timing of each species and their relationship with both temperatures and nutrients (amongst other parameters) in different time-series across

554   the world ocean. Therefore, here we also used this grouping to compare and complete this
555   classification from a new time-series dataset.

556   *Globorotalia inflata* is the most abundant taxon in our samples. Our data shows that maximum
557   fluxes and relative abundances of this species are reached during winter and the winter-spring
558   transition (Figure 3). The relative abundances showed strong positive and negative significant (p
559   <0.05) correlations with the chlorophyll-*a* concentration and the SST: 0.808 and -0.896 respectively
560   (Figure 5). It is a non-spinose species and is considered a deep dweller (Hemleben et al., 1989;
561   Schiebel and Hemleben, 2017). Generally regarded as showing limited opportunistic behaviour and
562   it has been often associated with eddies and hydrological fronts (Chapman, 2010; Retailleau et al.,
563   2011). Concerning the Mediterranean, its maximum stocks and abundances have been recorded
564   along the southern margin of the western Mediterranean basin (Azibeiro et al., 2023), especially
565   during winter (Bárcena et al., 2004; Pujol and Grazzini, 1995; Rigual-Hernández et al., 2012); while
566   it is poorly represented in the eastern part, even absent in the Levantine basin (Avnaim-Katav et al.,
567   2020). As a consequence, *G. inflata* can be considered as a mesotrophic species, which is dominant
568   in regions with some degree of stratification of the water column and an intermediate amount of
569   nutrients and it has been used as a tracer of the Atlantic inflow in the Mediterranean basin (Azibeiro
570   et al., 2023), which agrees with the local hydrography in the Sicily Channel during winter and spring.
571   As *G. inflata* appeared in periods of cool and nutrient enriched waters (Figure 3), which coincide
572   with the periods of higher MAW influence in the Sicily Channel (Béranger et al., 2004), we consider
573   that our results further confirm *G. inflata* as tracer of the MAW in the Sicily Channel.

574   *Globorotalia truncatulinoides* is the second most abundant species in our record. However, our CCA
575   results suggest that the seasonal variations in *G. truncatulinoides* are not directly correlated with
576   either chlorophyll-*a* concentration or SSTs (r= -0.162 and 0.256, respectively, p >0.05) (Figure 5).
577   This highlights the fact that environmental controls other than the ones considered here may be
578   affecting its distribution. This taxon is a cosmopolitan species found in all major oceans (Schiebel
579   and Hemleben, 2017) and is considered a deep dweller with an affinity for water-mixing conditions
580   (Margaritelli et al., 2020; Schiebel and Hemleben, 2005). It is a non-spinose species with a complex
581   life cycle. In the Mediterranean, peak abundances of this species are found in the northwestern part
582   of the basin, where it represents a major component of the assemblages (Pujol and Grazzini, 1995;
583   Rigual-Hernández et al., 2012), while it is absent in the easternmost part of the basin (Avnaim-Katav
584   et al., 2020). This species has been documented to have a complex life cycle and reproductive
585   strategy. *G. truncatulinoides* has been described to reproduce once a year in the upper layers of the
586   water column, generally when the water mixing allows the migration of juvenile individuals to the
587   surface (Lohmann and Schweitzer, 1990; Schiebel et al., 2002). Then, adult individuals migrate
588   downward the water column and spend the rest of their life cycle (Rebotim et al., 2017; Schiebel
589   and Hemleben, 2005). Hence, we speculate that these complex migratory patterns may be playing
590   a role here. As its reproduction cycle is mainly controlled by the gametogenesis process, and as
591   described previously, it reproduces once a year (a slower rate than the majority of the planktonic
592   foraminifera species) (Schiebel and Hemleben, 2017), then, although different stages of its life cycle
593   could be affected by SST and chlorophyll-*a*, this is not necessarily registered by the sediment traps
594   in every stage of its growth.

595 *Globigerina bulloides* was the third most abundant planktonic foraminifera species identified here.
596 It is a surface to subsurface dweller and one of the most common species across the world ocean
597 (Schiebel and Hemleben, 2017). Interestingly, our analysis showed no significant correlation
598 between changes in *G. bulloides* relative abundance and chlorophyll-*a* concentration or SST (r= -
599 0.145 and -0.111 respectively, *p* >0.05). However, across the time span studied, this taxon showed
600 its maximum abundance and fluxes during relatively high chlorophyll-*a* and cool SST conditions
601 (Figure 3). This highlights that other environmental parameters than the ones considered here might
602 be playing a role in its distribution. It is a spinose species known for its opportunistic feeding strategy
603 (Schiebel et al., 2001) and affinity for upwelling and eutrophic environments (Azibeiro et al., 2023;
604 Bé et al., 1977). Within the Mediterranean Sea, it displays peak export fluxes to the deep sea in
605 areas of high productivity such as the Gulf of Lions and the Alboran Sea during the high productivity
606 period in late winter to spring (Azibeiro et al., 2023; Bárcena et al., 2004; Hernández-Almeida et al.,
607 2011; Rigual-Hernández et al., 2012), while few individuals are found in the eastern part of the
608 Mediterranean (Avnaim-Katav et al., 2020). We surmise that owing to its multiple trophic strategies
609 and its multi-diet characteristics, it could adapt and feed on varying chlorophyll-*a* concentrations.
610 Also, the lack of correlation with both parameters could be explained by the fact that this taxon is
611 associated with eutrophic conditions. In the Sicily Channel, the high productivity period ranges from
612 winter to spring, and the conditions allow deep mesotrophic dwellers (i.e. *G. inflata*) to dominate
613 the assemblage; while in summer and autumn, the upwelling setting brings oligotrophic conditions
614 that are not favourable for this species. In addition, the maximum abundances of *G. bulloides* are
615 displayed coincidently with the highest number of benthic foraminifera identified (see
616 Supplementary data), which in turn could mean that some of the *G. bulloides* specimens during their
617 maximum abundance have a resuspended origin.
618 Generally, both *G. bulloides* and *G. truncatulinoides* fluxes and abundances are positively linked to
619 favourable food conditions and high-productivity environments. The first species tends to exhibit a
620 "bloom" strategy on short time scales, while the second species tends to be related to nutrient
621 advection zones in the Mediterranean Sea (Margaritelli et al., 2022). Furthermore, in the
622 Northwestern Mediterranean a previous study showed that the fluxes of these two species are
623 almost in phase (Rigual-Hernández et al., 2012). Interestingly, in the Sicily Channel, this relation is
624 not straightforward. In the Gulf of Lions, *G. bulloides* is the main species and shows the classical
625 "bloom" behaviour, while *G. truncatulinoides* pattern is more constant and its variations are more
626 gradual (Rigual-Hernández et al., 2012). Although the timing of the two species is different in our
627 record, the response of *G. truncatulinoides* is similar across the record. Furthermore, from a
628 productivity standpoint, the Sicily Channel is less productive than the Gulf of Lions (Siokou-Frangou
629 et al., 2010), which, in turn, does not benefit *G. bulloides* abundances and, as the upwelling in our
630 study zone is less pronounced than in other parts of the Mediterranean, the timing between the
631 two species is different. Additionally, the intensity of the upwelling in the central Mediterranean is
632 controlled by variations in the intensity of the LIW flowing to the western part of the basin (Astraldi
633 et al., 2001; Lermusiaux and Robinson, 2001; Pinardi et al., 2015), with higher intensity leading to
634 reduced upwelling and therefore, productivity. This could explain the lack of high abundance of *G.*
635 *bulloides* in our study region as the upwelling in the Sicily Channel is reduced compared to other
636 places in the Mediterranean (D'Ortenzio, 2009; Siokou-Frangou et al., 2010) and therefore, the

637 increase in productivity is diminished compared to other regions in which the productivity and the
638 abundance of *G. bulloides* are higher, such as the Alboran Sea (Bárcena et al., 2004). Therefore, we
639 consider that a combination of ecological preferences and oceanographic processes could explain
640 the lack of synchronicity between these two species fluxes and abundances.
641 *Globigerinoides ruber* and *G. ruber* (pink) were the fourth and fifth most abundant species in our
642 samples (Table 1). Our correlation analyses showed a significant positive effect of SST (r= 0.803 and
643 0.678, *p* <0.05) and a significant negative effect of chlorophyll-*a* (r= -0.567 and -0.464 respectively,
644 *p* <0.05) on both *G. ruber* and *G. ruber* (pink) respectively (Figure 5). These species have been
645 described as tropical to subtropical taxa, with an affinity for oligotrophic and stratified waters (Bé
646 et al., 1977). Both of these species are among the shallowest dwellers of the extant planktonic
647 foraminifera species and are considered one of the most adaptable to varying surface water
648 conditions (Kemle-von Mücke and Oberhänsli, 1999; Schiebel and Hemleben, 2017). Due to its
649 temperature and salinity limits for food acceptance, the white variety is one of the most studied
650 foraminifera species in culture experiments, which highlight their euryhaline and eurythermal life
651 cycle (Bijma et al., 1990; Lombard et al., 2009). In today's ocean, the white variety is substantially
652 more abundant than the pink one (Schiebel and Hemleben, 2017). In the case of the Mediterranean
653 basin, *G. ruber* is generally associated with warm and oligotrophic waters (Pujol and Grazzini, 1995)
654 and is abundant in the eastern oligotrophic basin, where it dominates the assemblages in the
655 Levantine basin during spring and fall (Avnaim-Katav et al., 2020). However, although present in the
656 western basin, its abundance is much lower in the Gulf of Lions (Rigual-Hernández et al., 2012) and
657 in the Alboran Sea (Bárcena et al., 2004). Overall, the correlation data agrees with the previous work
658 that linked *G. ruber* (both varieties) to warm and oligotrophic conditions generally displayed during
659 a higher stratification of the water column (Schiebel et al., 2004). As this species is mostly abundant
660 in the eastern part of the Mediterranean , it should be expected that the LIW, when it dominates
661 the circulation during summer and autumn, brings this species along with other oligotrophic taxa.
662 However, fluxes (Figure 3) and relative abundance data (supplementary Figure 3) showed that this
663 species maximum appearances were recorded during winter, coincidently with *G. inflata* and *G.*
664 *truncatulinoides*. Therefore, the winter recorded in our dataset showed favorable conditions for
665 both deep mesotrophic dwellers and oligotrophic species such as *G. ruber*. We interpret this pattern
666 as a reduced influence of the MAW during winter in the Sicily Channel that could lead to slightly
667 warmer than usual surface conditions that favor the stratification and hence, the *G. ruber*
668 abundances. Concerning *G. ruber* (pink), as its fluxes and abundances were higher during summer,
669 and it is mainly identified in the eastern part of the Mediterranean as well, we consider that the LIW
670 influence bring this species in the Sicily Channel. ~~as they appear mainly during summer and autumn,~~
671 ~~coincidently with the increased LIW and eastern basin waters influence in the Sicily Channel~~.
672 According to Jonkers and Kučera, (2015), the foraminifera fluxes can be predicted on a seasonal
673 scale for three different groups of planktonic foraminifera. Following this approach, we explore the
674 relative abundance of these three aggrupations to document if these correlate with both SST and
675 chlorophyll-*a* concentration (see Supplementary Table 1) on the period covered by the sediment
676 trap (Figure 5). The first group (group 1) consists of both *G. ruber* varieties, *G. sacculifer*, *O. universa*,
677 *G. siphonifera*, *G. rubescens* and *G. tenella*. The second group (group 2) is formed by *G. bulloides*, *T.*
678 *quinqueloba*, *N. incompta*, *G. scitula* and *G. calida*. In our record, however, either *G. bulloides* or *G.*

679 *calida* displayed a similar trend, and the remaining three species abundance was <1.5%, making any
680 significant assumption difficult (Table 1). The third (group 3) is composed by the deep dwellers *G.*
681 *inflata* and *G. truncatulinoides*. Group 1 showed a strong and significant positive correlation with
682 the SST (Figure 5) and a negative with the chlorophyll-*a* (r= 0.828 and -0.668 respectively, *p* <0.05,
683 see Supplementary Table 1). This is not surprising as the majority of the group is formed by species
684 not only considered tropical but also well adapted to oligotrophic and nutrient impoverished
685 environments (Chapman, 2010; Hemleben et al., 1989; Schiebel and Hemleben, 2017). In addition,
686 most components of this group are symbiont bearing species (Takagi et al., 2019), which have been
687 described to be more adapted to nutrient depleted and oligotrophic conditions. Group 2 on the
688 other hand did not show any strong correlation to either SST and chlorophyll-*a* concentration,
689 although a significant negative correlation was displayed between the group abundances and the
690 latter parameter (r= -0.525, see Supplementary Table 1). This result is not surprising as the main
691 component of this group is *G. bulloides*, which previously showed a lack of correlation with both SST
692 and chlorophyll-*a*, while the remaining species of this group were taxa that tend to be outnumbered
693 by more opportunistic species (i.e. *N. incompta* and *T. quinqueloba*) (Kuroyanagi and Kawahata,
694 2004; Schiebel, 2002). Also, the overall abundance of these taxa was very low in our samples
695 compared to the other two groups, which in turn could affect the correlation results. Here we
696 propose that the mesotrophic conditions of the Sicily Channel developed during the relatively high
697 productivity period are not favourable enough for the development of the taxa comprised in group
698 2. Finally, group 3 displayed a strong and significant positive correlation with chlorophyll-*a*
699 concentration (r= 0.771, *p* <0.05), which is an expected trend according to the affinity showed to
700 mesotrophic conditions by the two species that constitute this group, however, as compared to
701 Jonkers and Kučera, (2015), we showed a strong and significant negative correlation of these two
702 species abundances with the SST (Figure 5). The latter work stated that the cycles of these species
703 were independent of the temperature changes, however, these two species tend to be used as
704 tracers of cool and deep mesotrophic waters in the Mediterranean, generally associated with the
705 MAW (Azibeiro et al., 2023).
706 In summary, our data showed that in the Sicily Channel, the three major ecological groups proposed
707 by Jonkers and Kučera, (2015), exhibited a different response to environmental variability. Overall,
708 groups 1 and 3 showed significant correlation with the latter parameters and were in accordance
709 with their corresponding species ecologies. However, group 2 did not show any significant
710 correlation, which we interpreted as the result of very low abundances of the taxa comprised within
711 this group. This translates into the dominance of group 1 during summer and autumn when
712 oligotrophic and warm eastern waters dominate the water column, while the mesotrophic taxa from
713 group 3 dominate during winter and spring, coincidently with higher primary productivity, yet not
714 eutrophic enough for the opportunistic taxa comprised in the group 2, which is less well represented
715 in the Sicily Channel.
716
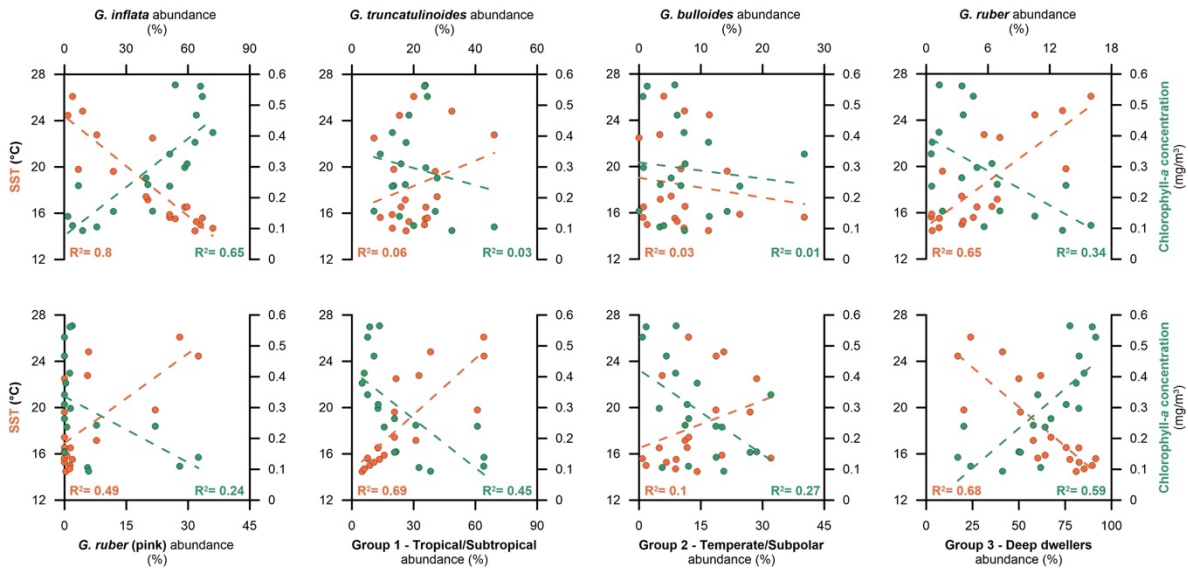
Figure 5. SST and chlorophyll-*a* concentration against the relative abundance of the five most abundant species and the three ecological groups proposed by Jonkers and Kučera (2015). Orange dots stand for SST while the green ones correspond to chlorophyll-*a*.

5.3. Influence of the hydrodynamic conditions on the planktonic foraminifera assemblage

A possible source of variability between the living foraminifera assemblages and those collected by the trap could be the preferential transport of certain species by the currents as well as differences in the sinking rates between species. Typically, deep dwelling species produce heavier shells that the surface dwelling ones (Zarkogiannis et al., 2022). Theoretically, lighter species are easier to remobilize than the heavier ones, however, if the current is strong enough, lighter species could travel far away while heavier species could be reworked in the vicinity of their deposition zone. *G. truncatulinoides* is among the heaviest planktonic foraminifera species (Beer et al., 2010; Béjard et al., 2023). Therefore, if the current is strong enough, it could be resuspended and be recorded by the sediment trap. The record in the seabed sediment (see section 5.5) showed that *G. truncatulinoides* was more abundant in the settling particles from the C01 mooring line (Figure 8), and according to the winnowing theory, *G. inflata* should follow a similar pattern as it also a heavy species (Zarkogiannis et al., 2022). However, surface data (Mallo et al., 2017) showed that the latter is also the dominant species in the BONGO nets (see section 5.5). Furthermore, Takahashi and Be, (1984) presented the data about the sinking speeds of different planktonic foraminifera species. As an example, *G. inflata* showed a sinking speed of 500 m per day, compared to 330 m per day for *G. bulloides*. These different sinking rates applied in a water column of around 450 m suggest that the likely origins of the planktonic foraminifera collected by the traps must be similar and are insufficient to generate discrepancies between the foraminifera assemblages living in the upper water column and those collected by the trap.
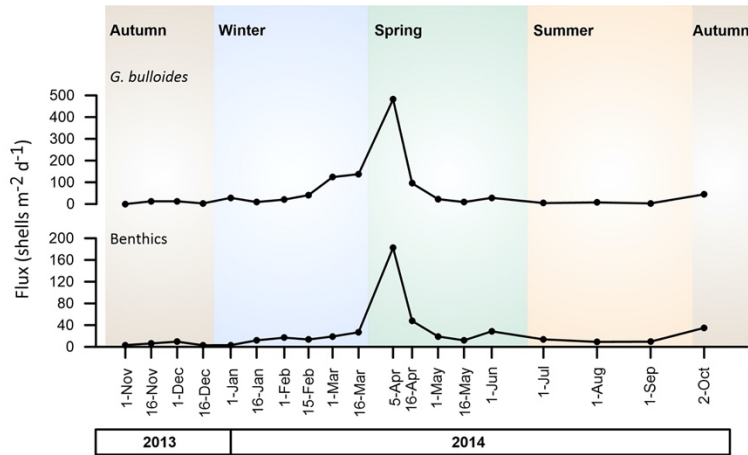
Figure 6. *G. bulloides* and benthic foraminifera fluxes (shells m^{-2} d^{-1}) between November 2013 and October 2014.

The identification of benthic foraminifera individuals highlights suggest an impact of the hydrodynamic conditions on the settling particles populations. The main species identified were *T. saggitula* spp. and *B. marginata* (Plate 1) along with a small number of *Uvigerina mediterranea* and *Lagenina striata*. These taxa are considered infaunal species, i.e. they live buried in the sediment (Balestra et al., 2017; Milker and Schmiedl, 2012) and are commonly found in continental shelves and slopes. Overall, benthic foraminifera accounted only for a mean of 3.4% of the total foraminifera identified in the C01 settling particles (Table 1) and the percentage of planktonic oscillated between 89 and 99.4%. Most of the annual benthic fluxes occurred during April, when a total of 80% of the annual benthic foraminifera fluxes were recorded (Figure 6). As described previously, the Sicily Channel hydrography is complex from both a vertical and seasonal point of view (Astraldi et al., 2001; Garcia-Solsona et al., 2020; Incarbona et al., 2011; Pinardi et al., 2015; Schroeder et al., 2017). In the Sicily Channel, the tidal and subtidal current speed is known to reach maximum annual values during the spring period (Gasparini et al., 2004) which could be invoked as a possible source of sediment resuspension including benthic species. This has also been observed in different parts of the Mediterranean (Grifoll et al., 2019). Indeed, in our record, the highest benthic foraminifera fluxes were collected during spring (Figure 6), i.e. the period of peak current intensity in the Channel. Coincidently, it also showed the highest fluxes of *G. bulloides* (Figure 3), which is the third most abundant species in our record (Table 1). Interestingly, this species annual flux distribution showed no correlation with either the SST nor the chlorophyll-*a* (Figure 5). These observations, coupled with the fact that the fluxes of *G. bulloides* and the benthic foraminifera were positively and significantly correlated (r= 0.89, *p*<0.05), suggest that benthic species were resuspended, being caught at 40 m of water depth by our sediment trap. Furthermore, a low number of detritic debris, such as mica flakes, were identified in the samples that contained the highest number of benthic foraminifera (April 2014), which again suggest a secondary influence of resuspended sediments in the sediment trap record in specific intervals of the annual cycle. However, no such relationship has been identified with the other species that did not show any correlation with the previous environmental parameters: *G. truncatulinoides*. Consequently, we hereby propose that *G. bulloides* distribution and abundances are blurred in specific intervals by the resuspension of sea floor sediments. Finally,

776 the increase of *G. bulloides* abundance and fluxes that has been identified coincidently with a higher
777 number of benthic foraminifera during early April could lead to the interpretation that the benthic
778 foraminifera are the result of the intensification of the MAW. However, as the presence of the
779 benthic foraminifera is patchy and not constant, we do not consider their presence is ruled out as a
780 reliable proxy for the MAW/LIW intensity. Therefore, it can be concluded that the C01 sediment
781 trap mainly records a pelagic signal with a secondary influence of resuspended sediments.
782

783 **5.4 Geographical variability in the magnitude and composition of planktonic foraminifera fluxes**
784 **across the Mediterranean**
785 The comparison of the settling planktonic foraminifera assemblage ~~sediment trap~~ from the Sicily
786 Channel with the ones retrieved from different parts of the Mediterranean offers a unique
787 opportunity to provide further insight into the central Mediterranean dynamics and ecology of this
788 group.
789 As stated previously, the planktonic foraminifera flux in the Sicily Channel was higher from mid-
790 January to mid-March, which coincided with the highest chlorophyll concentrations and the coolest
791 SST recorded (Figure 2). This seasonality is similar to the one observed in the Gulf of Lions, where
792 the planktonic foraminifera flux reached its highest values from mid-February to mid-March during
793 different years (Rigual-Hernández et al., 2012). Although slightly different, the planktonic
794 foraminifera fluxes patterns from both the Levantine basin and the Alboran Sea also displayed
795 maximum values between mid-February to mid-March and mid-January to mid-February
796 respectively (Avnaim-Katav et al., 2020; Hernández-Almeida et al., 2011). However, the magnitude
797 of the planktonic foraminifera flux values displayed some differences between the sites (see
798 Supplementary Figure 2). Overall, for the Sicily Channel, values ranged between 0-1889 shells m^{-2} d^{-1}
799 ^{1} with a mean value of 629 shells m^{-2} d^{-1}. These values were comparable to the ones from the Gulf
800 of Lions: 0-2114 and 4268 shells m^{-2} d^{-1} with a mean value of 225.4 in Planier sediment trap to 419
801 shells m^{-2} d^{-1} in Lacaze-Duthiers sediment trap (Figure 7). On the other hand, the Levantine basin
802 values were lower: 0-429 shells m^{-2} d^{-1}, with a mean value of 93 shells m^{-2} d^{-1}. Finally, the highest
803 values belonged to the Alboran Sea: 0-6000 shells m^{-2} d^{-1} with a mean value of 783 to 970 shells m^{-2} d^{-1}
804 ^{2} d^{-1} depending on the gyres. Note that the planktonic foraminifera flux values from the Levantine
805 basin used here represent the foraminifera shells from the >125 μm fraction, which highlights the
806 fact that compared to the >150 μm, the flux values should be even lower. The corresponding
807 chlorophyll-*a* values registered in the latter sites were 0.2-0.65 mg m^{-3} for the Sicily Channel (Figure
808 5), 0.25-0.85 mg m^{-3} for the Gulf of Lions (0-0.65 mg m^{-3} in the Planier site, 0.25-0.85 mg m^{-3} for
809 Lacaze-Duthiers) (Rigual-Hernández et al., 2012), 0.02-0.4 mg m^{-3} for the Levantine basin (Avnaim-
810 Katav et al., 2020) and 0.1-1.2 mg m^{-3} in the Alboran Sea (Hernández-Almeida et al., 2011), indicating
811 a similar productivity in terms of chlorophyll-a between the Gulf of Lions and the Sicily Channel. In
812 addition, here we calculated an annualized planktonic foraminifera flux (section 3.4) for each of the
813 6 sites compared here (Figure 7). Overall, the highest annualized fluxes were displayed in the
814 Alboran Sea (Figure 7): around 3x10^{5} and 4.4x10^{5} shells m^{-2} y^{-1}, while the lowest one was displayed
815 in the Levantine Basin: a little over 30000 shells m^{-2} y^{-1} (Figure 7). The Gulf of Lions and the Sicily
816 Channel displayed comparable annualized fluxes although higher for the latter: around 1.5x10^{5} and
817 1.85x10^{5} shells m^{-2} y^{-1} respectively. Note that PLA site values were significantly lower: around 7x10^{4}

818   shells m^{-2} y^{-1} (Figure 7). Previous work showed that these planktonic foraminifera patterns were
819   mainly linked to specific regional oceanographic processes. First of all, the Levantine basin is well
820   known for being an ultra-oligotrophic region and being the warmest and saltiest of the
821   Mediterranean basins (Ozer et al., 2017), mainly due to the W-E anti-estuarine circulation. On the
822   other hand, the Gulf of Lions is considered an exception to the general oligotrophy of the
823   Mediterranean. Seasonal vertical mixing phenomenon occurs in winter, generated by cold winds.
824   This winter mixing recharges the surface waters with nutrients, allowing a winter/spring productivity
825   bloom (Durrieu de Madron et al., 2013; Houpert et al., 2016). Finally, the Alboran Sea is a transitional
826   region between the Atlantic Ocean and the Mediterranean Sea (Hernández-Almeida et al., 2011),
827   and unlike the latter, is not an oligotrophic region due to the two systems of high productivity
828   related to the gyres generated by an intense westerlies activity, which allow nutrients enriched
829   (compared to the resident waters) Atlantic waters to spread into the Mediterranean. This results in
830   an enhanced primary productivity period from November to March. According to the PFF patterns
831   displayed in this study, the Sicily Channel presents similar values and fluxes distributions to the Gulf
832   of Lions, however, its oceanographic circulation is significantly different from the latter. These
833   observations agree with the work of Mallo et al., (2017) carried out with plankton tows in the whole
834   Mediterranean basin. The latter work found that the Alboran Sea displayed the highest standing
835   stocks of planktonic foraminifera, while the easternmost part of the Mediterranean showed the
836   minimum values. Also, the Gulf of Lions and the Channel of Sicily displayed similar stocks, although
837   slightly superior for the Channel of Sicily.
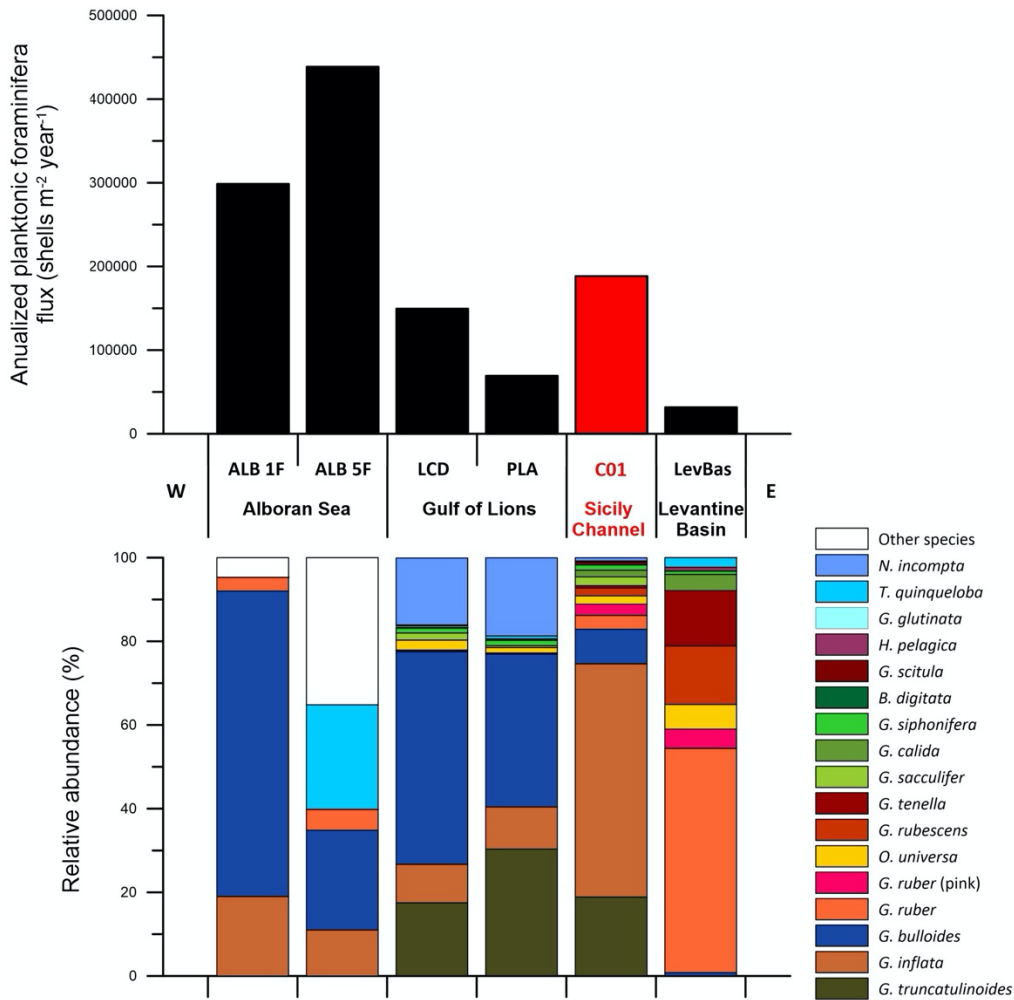
838

839 **Figure 7.** Comparison of the annualized (see section 3.4) planktonic foraminifera flux and the relative
840 abundance of each species identified in different time-series across the Mediterranean Sea (see section
841 3.5). The data from the Sicily Channel (C01) is depicted in red. Note that the Levantine Basin (LevBas)
842 dataset covers the >125 μm fraction. Other species (white bar) in the Alboran Sea corresponds to any
843 species different from the main 4 taxons identified in Bárcena et al., (2004) and Hernández-Almeida et
844 al., (2011).

845

846 Concerning the species composition, we identified 15 planktonic foraminifera species in the Sicily
847 Channel, which is a similar species number to the one from the Gulf of Lions (14 species) and higher
848 than in the Levantine basin (10 different species). The Sicily Channel site displayed the highest
849 planktonic foraminifera assemblage diversity among the three sites compared: a mean 1-D and S/W
850 index of 0.68 and 1.57 respectively. (Table 2). Interestingly, despite showing a similar number of
851 different species, the Gulf of Lions displayed the lowest diversity values, especially for the PLA site:
852 mean 1-D of 0.55 and mean H/W of 1.08, while the LCD site 1-D and h/w were 0.58 and 1.15
853 respectively. These observations highlight that, although the annualized planktonic foraminifera flux
854 was similar between the Gulf of Lions (for the LCD site) and the Sicily Channel (Figure 7), the
855 assemblage in the latter site was significantly more diverse regarding species composition. The

856   composition of the annual planktonic foraminifera population of the different species showed some
857   differences between the sites compared here. In the Levantine basin, the majority of the planktonic
858   foraminifera population consisted of surface symbiont bearing species such as *G. ruber*, *G. ruber*
859   (pink), *G. rubescens*, *G. tenella*, *O. universa*, which are well adapted to the ultra-oligotrophic
860   conditions (Lombard et al., 2011; Schiebel and Hemleben, 2017). The latter species represented 96%
861   of the total planktonic foraminifera in the Levantine basin, while the same species in the Sicily
862   Channel accounted for around 10% of the total individuals (Figure 7). Note that both *G. rubescens*
863   and *G. tenella* are considered small-sized species (Chernihovsky et al., 2023) and their adult size is
864   often smaller than 150 μm, so it is possible that some individuals of those species may not be
865   recorded in our data. On the other hand, in the Gulf of Lions, the four main species were *G. bulloides*,
866   *N. incompta*, *G. inflata* and *G. truncatulinoides*, which represented 88 to 95% of the total planktonic
867   foraminifera (Rigual-Hernández et al., 2012). These species tend to be associated with eutrophic to
868   mesotrophic environments which coincides with the Gulf of Lions locally enhanced primary
869   productivity conditions. In the Sicily Channel, the same species accounted for 83% of the total
870   individuals, and, except for *N. incompta*, the remaining three species were also the most abundant
871   in our samples.

872

873   **Table 2.** Inverse Simpson (1-H) and Shannon-Weiner indexes mean, standard deviation ("Stan. Dev.")
874   and maximum values for the two Gulf of Lions sites (PLA and LCD), the Sicily Channel (C01, this study)
875   and the Levantine Basin (LevBas).

	Gulf of Lions		Sicily Channel	Levantine Basin
	LCD	PLA	C01	LevBas
Simpson 1-H				
Mean	0.581	0.553	0.681	0.615
Stan. Dev.	0.168	0.180	0.132	0.144
Max	0.802	0.781	0.872	0.804
Shannon H/W				
Mean	1.151	1.078	1.572	1.230
Stan. Dev.	0.359	0.375	0.398	0.316
Max	1.789	1.630	2.188	1.759

876

877   Considering the planktonic foraminifera fluxes patterns, the species diversity and the planktonic
878   foraminifera most abundant species from each of the three Mediterranean time-series with which
879   we compared our data, we interpret that, from a planktonic foraminifera population point of view,
880   the Sicily Channel could be considered as a transition zone and a biological corridor between the
881   western and eastern basins.

882

883   Finally, to put our data into a global context, here we compare our dataset with planktonic
884   foraminifera data from the same size fraction retrieved in the Gulf of Mexico, high latitudes North
885   Atlantic and gyres region of the North Atlantic Ocean. In the northern Gulf of Mexico, from 2008 to
886   2010, the >150 μm PFF was comprised between 0 and slightly over 800 shells $m^{-2} d^{-1}$, with a mean

887 value of around 250 shells $m^{-2} d^{-1}$ (Poore et al., 2013). A total of 12 species were identified, with *G.*
888 *truncatulinoides*, *G. ruber* (pink) and *N. dutertrei* as the most abundant species recorded. On the
889 other hand, in the North and high-latitudes Atlantic Ocean, Wolfteich (1994), showed that the PFF
890 oscillated between 0 and around 5000 shells $m^{-2} d^{-1}$ for a mean value of 800 shells $m^{-2} d^{-1}$, while *G.*
891 *bulloides* and *N. incompta* were the most abundant species. Although the latter work only focused
892 on the most abundant species, additional work has documented more than 20 species in the vicinity
893 of the North-Atlantic gyres (Salmon et al., 2015), but around only three to four in the high latitudes.
894 This highlights that, from a planktonic foraminifera population point of view on a wider scale, the
895 Sicily Channel displayed a higher planktonic foraminifera flux and species richness compared to the
896 tropical to subtropical Gulf of Mexico and to the high latitudes of the North Atlantic, but lower values
897 compared to the North Atlantic gyres region.
898
899 **5.5 Recent planktonic foraminifera assemblage comparison with seabed sediment**
900
901 The Mediterranean Sea is often referred to as a climate change hotspot and a "laboratory basin" where
902 many global environmental trends are amplified (Bethoux et al., 1999). In particular, ocean warming is
903 expected to exceed the global average (Hassoun et al., 2022, 2015; Lazzari et al., 2014) while it is
904 considered a specially sensitive zone of the ocean to acidification due to the fast turnover of its waters
905 and penetration of anthropogenic CO_2 (Bethoux et al., 1999; Schneider et al., 2007). One of the main
906 questions about planktonic foraminifera concerns the way they are going to react to the ongoing climate
907 change in the global ocean (Jonkers and Kučera, 2015; Schiebel and Hemleben, 2017). Previous work
908 suggests that global communities of planktonic foraminifera have already been affected by
909 environmental change since the onset of industrialization (Jonkers et al., 2019). Moreover, recent work
910 has shown that the calcification of several planktonic foraminifera species has decreased during the
911 industrial era in the northwestern Mediterranean (Béjard et al., 2023). Therefore, here we aim to assess
912 if modern planktonic foraminifera communities dwelling in the Sicily Channel differ from their pre-
913 industrial counterparts. To do so, next, we compare the annual integrated assemblages collected by the
914 sediment trap in the C01 mooring line with the ones from a set of core-tops, two box-cores and BONGO
915 nets retrieved in the vicinity of the studied zone (see Section 3.5).
916 As planktonic foraminifera are a group of calcifying plankton, when comparing sediment trap and
917 seabed sediment data, the possible role of calcite dissolution must be discussed. Firstly, the
918 Mediterranean Sea is supersaturated with respect to calcite (Álvarez et al., 2014; Millero et al., 1979)
919 and the depth of the studied material is substantially shallower than the calcite saturation horizon
920 (Álvarez et al., 2014). Secondly, recent work suggests that calcite experiences little to negligible
921 changes in the water column and burial in recent sediments (Béjard et al., 2023; Pallacks et al.,
922 2023). All this evidence suggests that dissolution played a negligible role in the preservation of
923 planktonic foraminifera preserved in the sediment record in the study region.
924 The core-tops used for comparison were part ~~with which the C01 sediment trap data is compared~~
925 ~~were part~~ of the MARGO database (see Section 3.5 for more details). Note that the MARGO sites
926 3735 to 3739 seabed sediment was taken using a trigger-weight corer (Thunell, 1978). However,
927 samples 3658, 3672 and 3673 were retrieved using a piston corer (Hayes et al., 2005). Generally,
928 sampling with the trigger-weight method is considered to retrieve less mixed and disturbed

sediment than the piston or box corer sampling methods (Skinner and McCave, 2003; Wu et al., 2020). Therefore, the foraminifera assemblages from the core-tops may likely represent a mix of Holocene populations rather than exclusively modern assemblages. Although the lack of dating control makes it impossible to determine the exact date of the core top assemblages. , our data suggest that the composition of modern foraminifera assemblages in the Sicily Channel has changed between the late Holocene and the present day.

The sites 342 and 407, studied by Incarbona et al., (2019), were retrieved with a box-corer. A total of 23 and 24 samples were analyzed in the latter work, respectively. The advantage of comparing the C01 assemblages with those of Incarbona et al., (2019) is the availability of high resolution ^{210}Pb chronology. The ages ranged from 1718 to 1962 CE for site 342 and from 1558 to 1994 CE for site 407. Therefore, here we present a comparison with the mean relative abundance of the main planktonic foraminifera species from all the samples available (Figure 8).

Finally, to provide a more complete snapshot of the surface assemblages, we also include the abundances from Mallo et al., (2017) that were collected with a BONGO net during spring 2013 in the axis of the Sicily Channel (Figure 8).

The reasons of this change are uncertain, although we speculate that ongoing warming (Lazzari et al., 2014), the consequent increasing stratification of the water column in the Mediterranean (Siokou Frangou et al., 2010) and a shift in the oceanographical configuration could have already reduced primary production in the Sicily Channel.

In terms of planktonic foraminifera assemblage composition, major differences were observed between the different seabed sediments datasets (Figure 8). Overall, the settling population from the C01 mooring line appeared to be closer to the assemblages from sites 342 and 407 (Figure 8) than to the mean from the MARGO database (see Supplementary data). The most evident observation relies on the shift of the dominant species when comparing the settling population with the sites 342, 407, the BONGO net and the core-top assemblages (Figure 8). As described previously, *G. inflata* dominated the assemblages collected by the sediment trap (Table 1). This is also the case for the sites 342 and 407 and the BONGO net (Figure 8). However, *G. bulloides* was the best-represented species in the core-tops from the MARGO database. Also, the second most abundant species varied across the datasets: *G. ruber* in the sites 342 and 407, *O. universa* in the BONGO nets and *G. inflata* in the MARGO core-tops, with abundances around 27-29, 29 and 27.5%, respectively. ollowed by *G. inflata* and *G. ruber* (Figure 8). The latter species showed mean relative abundances of 27.5%, 23% and 20% across all core-tops, respectively. Interestingly, *G. truncatulinoides* abundance was significantly lower in the seabed datasets and absent in the BONGO nets, highlighting the deep aspect of its ecology (Figure 8). On the other hand, the "other species" category, which consists of minor taxa such as *G. rubescens, G. siphonifera* and *G. calida* (amongst others) played a more significant role in the MARGO core-tops and BONGO nets assemblages, reaching abundances up to 26% (Figure 8), while in the sites 342 and 407, these species abundances are similar to those of the sediment trap.

These results lead to several observations. Firstly, *G. bulloides, considered more susceptible to dissolution than the average planktonic foraminifera species (Dittert et al., 1999), dominates the seabed sediment assemblages; and G. inflata, considered a less dissolution susceptible species (Schiebel and Hemleben, 2017) dominates the sediment trap population. This information*

971 ~~reinforces the idea that calcite dissolution in the water column or sediments is negligible. In other~~
972 ~~words, if dissolution was to take place here, *G. inflata* would be overrepresented in the seabed~~
973 ~~sediment, which is not the case.,~~ concerning the seabed sediment comparison, the sediment trap
974 assemblage is closer to the sites 342 and 407 than to the MARGO database core-tops. The
975 comparison with the surface BONGO nets shows that, although the dominant species are the same
976 (i.e. *G. inflata*), the influence of *O. universa* and the overall diversity is less important in surface
977 waters. This highlights the complexity of the Sicily Channel configuration and the differences
978 between the surface (BONGO nets), the water column (sediment trap) and the seabed sediment
979 (MARGO database and sites 342 and 407) regarding the planktonic foraminifera populations.
980 Secondly, the seabed sediment planktonic foraminifera populations showed a reduced influence of
981 deep-dwelling species (excepting for *G. inflata* in sites 342 and 407) and a more pronounced
982 influence of both eutrophic and oligotrophic species. These eutrophic species (such as *G. bulloides*
983 but also *N. incompta*) are associated with MAW and western basins in the modern Mediterranean
984 Sea, while the more oligotrophic taxa (*G. ruber*, *G. rubescens*, *G. calida*…) are considered to be
985 abundant in the easternmost part of the basin (Azibeiro et al., 2023). As noted previously, although
986 the settling assemblage differs to the ones from the seabed sediment, it is more similar to the sites
987 342 and 407 than to the MARGO database core-tops. Also, the ^{210}Pb chronology available for sites
988 342 and 407 covers the years 1558 to 1994 CE (Incarbona et al., 2019). A possible interpretation of
989 these results is that the MAW influence into the basin may have shifted. Instead of bringing rich and
990 eutrophic waters that would allow the development of opportunistic species, it nowadays brings
991 more mesotrophic water masses that favour the development of deep dwellers in the Sicily Channel.
992 On the other hand, this could also lead to the assumption of a reduced eastward and LIW influence
993 in the present day as seen by the significantly lower abundance of oligotrophic species in the settling
994 assemblages. Also, a change in the environmental conditions could lead to the increase of deep
995 dwellers in substitution of eutrophic species such as *G. bulloides*. As described previously, the
996 Mediterranean Sea has already been described as a climate change "hotspot", therefore the already
997 documented ocean warming and the consequent stratification (Malanotte-Rizzoli et al., 2014;
998 Siokou-Frangou et al., 2010) could have led to unfavorable conditions for several taxa. A decrease
999 in the primary production might have caused a shift in the dominance of the opportunistic *G.*
1000 *bulloides* by *G. inflata*. As described previously, *G. bulloides* shows a high affinity for high
1001 productivity environments, while deep dwellers such as *G. inflata* and *G. truncatulinoides* tend to
1002 prefer mesotrophic and stratified waters. Finally, note that the high abundance of *G. bulloides* in
1003 the seabed sediment could also be the result of a punctual high productivity events. In the Alboran
1004 Sea, during upwelling events, big amounts of *G. bulloides* are deposited in the seabed and dominate
1005 the assemblages, which reduces the relative abundance of other mesotrophic taxa (Bárcena et al.,
1006 2004; Hernández-Almeida et al., 2011). Then, multiple recurring high productivity events occurring
1007 over time in the Sicily Channel could explain the amount of *G. bulloides* in both the MARGO core-
1008 tops and the sites 342 and 407. In that sense, the recent warming and stratification of the
1009 Mediterranean could explain the recent trend in the planktonic foraminifera population registered
1010 by the ~~C01~~ sediment trap. However, in that case, species such as *G. ruber* and other oligotrophic
1011 species should be at least as much represented as in the seabed sediment. Alternatively, this could

imply a change in the intensity of the water masses flowing, such as an increased mesotrophic MAW influence and a reduced oligotrophic LIW influence.

Additionally, from a chronological point of view, we propose that the main assemblage change between the settling and the seabed sediment assemblages (i.e. the dominance of *G. inflata*) took place during the late Holocene but preceded the industrial period. The Incarbona et al., (2019) dates showed that, overall, since 1558 CE, *G. inflata* already dominated the samples. Also, the chronology in the work from Margaritelli, (2020) coupled with the abundances presented in allowed to show that, since the Little Ice Age, the three dominant species in the western Sicily Channel are *G. inflata* followed by *G. ruber* and *G. bulloides*. This brings further confirmation that *G. inflata* dominated the seabed sediment in the late Holocene, but also to the fact that the shift in the secondary species (i.e. *G. truncatulinoides* instead of *G. ruber* and *G. bulloides*) is rather recent. Also, we assume that the discrepancy with the MARGO core-tops sample is the result of the low temporal resolution.
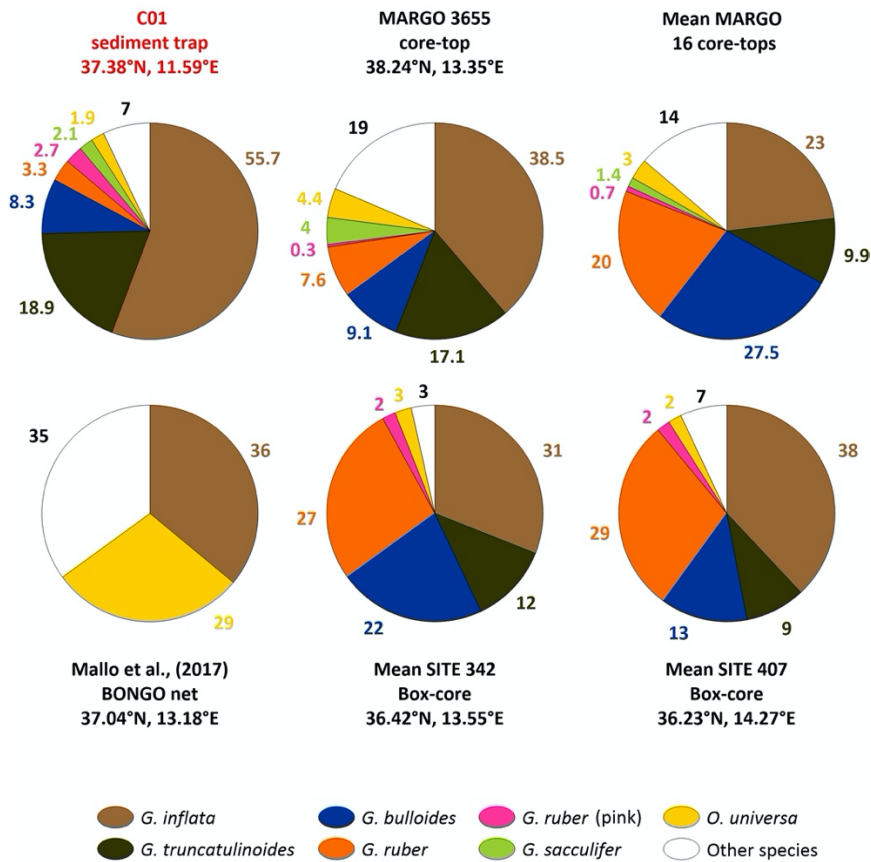
Figure 8. Comparison of the relative abundance of the planktonic foraminifera from the sediment trap and seabed sediment. From top left to bottom right: the settling assemblage from the sediment is depicted in red; MARGO site 3655 corresponds to the lowest squared chord distance; the mean relative abundance of all MARGO sites included in this study (see Supplementary data); the results from the BONGO net retrieved in the Sicily Channel from Mallo et al., (2017); finally, the mean abundances (see section 3.5) from the two sites presented in Incarbona et al., (2019): sites 342 and 407.

1033

1034   **Table 3.** MARGO core-tops analyzed, their latitude and longitude and the squared chord distance (SCD)
1035   between the sediment trap in the C01 mooring line and the MARGO database core-tops. The complete
1036   SCD for all sites can be found in Supplementary data.

	MARGO database															
Site	3655	3677	3724	3739	3737	3738	3658	3725	3654	3680	3735	3736	3673	3727	3661	3726
Latitude	38.25	36.47	35.85	36.73	38.33	38.00	36.68	36.49	38.22	37.46	38.17	38.23	39.40	38.93	39.41	38.64
Longitude	13.35	11.49	13.03	13.95	11.80	11.78	12.28	13.32	13.27	11.55	11.23	11.25	13.34	10.59	13.34	10.78
SCD to C01	0.27	0.52	0.55	0.56	0.66	0.78	0.84	0.85	0.88	0.89	0.90	0.93	1.03	1.03	1.07	1.10

1037

1038   To document the differences between the assemblage in the C01 mooring line and the MARGO
1039   database core-tops, we hereby analyze the SCD between the annual integrated settling foraminifera
1040   assemblage of the C01 mooring line and all the core-tops located in the Sicily Channel (see
1041   Supplementary Figure 2). Overall, the SCD ranged between 0.27 and 1.1 (Table 3). By using a
1042   dissimilarity coefficient value of <0.25 as cutoff criteria (see section 3.6 for more details), it can be
1043   concluded that none of the core-tops assemblages can be considered close analogues to the C01
1044   mooring line. The only exception might be MARGO site 3655, located around 180 km northeast of
1045   the mooring line, which displayed an SCD value of 0.27, very close to our cutoff threshold. ~~The mean~~
1046   ~~SCD between all core-tops and the sediment trap is 0.8, which contrasts with the SCD between the~~
1047   ~~core-tops, which exhibited an average value between them of 0.47 (see Supplementary data),~~
1048   ~~indicating a higher similarity between them than with the sediment trap.~~ Interestingly, from a
1049   geographical point of view, the geographical closest site analyzed (MARGO 3680) displayed a high
1050   SCD (0.89) despite being retrieved virtually in the underlying sediments beneath the C01 mooring
1051   line (Table 3). Overall, the 4 most similar sites (SCD <0.6) to the settling assemblage are all located
1052   eastward, while the 4 most different sites (SCD >1) are all located northward to the location of the
1053   mooring line. This highlights the geographical variability of the Sicily Channel regarding the
1054   planktonic foraminifera population and the complex oceanographic conditions. Note that, as
1055   mentioned previously, the lack of dating in these samples do not allow to bring further
1056   interpretations about the timing of planktonic foraminifera populations shifts. In addition to the lack
1057   of chronology control in these samples, no data is available for the sedimentation rate, which makes
1058   any assumption around the intensity of the hydrodynamics impossible. Finally, and as mentioned
1059   earlier, the retrieval method applied for the different core-tops could also be cited as source of the
1060   differences between the MARGO core-tops and with the sediment trap in the C01 mooring line.
1061   While a box-corer was used for sampling in sites 342 and 407 (Incarbona et al., 2019), various
1062   devices were used for the MARGO core-tops, that includes piston and gravity cores that are known
1063   to often experience stretching or loss of material during the recovery of the sediments. Therefore it
1064   is likely that the different MARGO surface sediment data set represent different time intervals. ~~We~~
1065   ~~speculate that the C01 sediment trap, in addition to registering species from both the western and~~
1066   ~~eastern Mediterranean basins, could also be considered a key point in an east to west planktonic~~
1067   ~~foraminifera population gradient. Interestingly, the most different core-tops are located in the~~
1068   ~~vicinity of the Tyrrhennian Sea and the most similar ones can be found in the easternmost part of~~

1069 ~~the Sicily Channel.~~ ~~In combination with the dominant taxa registered, we propose that the MAW~~
1070 ~~and western basin waters influence could have spread further east into the Sicily Channel. This, in~~
1071 ~~combination with the resident eastern basin waters, could reconcile the planktonic foraminifera~~
1072 ~~assemblage described from the C01 sediment trap and the fact that it is more similar to core-tops~~
1073 ~~located eastward.~~
1074 Taken into consideration all the uncertainties presented above, our data suggest that a change in
1075 the composition of the planktonic foraminifera assemblages took place at some stage of the late
1076 Holocene but before the onset of the industrial period. However, the available data precludes the
1077 determination of the main environmental drivers causing this change. ~~Overall, these results call for~~
1078 ~~increasing the monitoring of planktonic foraminifera populations and accentuating the comparisons~~
1079 ~~between recent and seabed sediment assemblages in the Mediterranean to determine if the trends~~
1080 ~~suggested by our data are the result of the recent environmental change.~~
1081
1082 **Conclusions**
1083
1084 The C01 mooring line, located on the axis of the Sicily Channel, provided the opportunity to
1085 document the planktonic foraminifera population on an interannual scale. We analyzed 19 samples
1086 that covered the timespan between November 2013 and October 2014. A total of 3723 individuals
1087 and 15 different species were identified. *G. inflata*, *G. truncatulinoides*, *G. bulloides*, *G. ruber* and *G.*
1088 *ruber* (pink) were the five most abundant species, representing 56, 19, 8, 3.5 and 3% of the total
1089 foraminifera. The remaining species represented less than 5% of the total individuals. Total
1090 planktonic foraminifera flux ranged between 44 and 1890 shells m^{-2} d^{-1}, higher values were reached
1091 during spring while values were lower during summer. Our data indicates that the planktonic
1092 foraminifera fluxes mainly reflect the oceanographic configuration of the Sicily Channel and its
1093 seasonal surface circulation variability. During winter and spring, a stronger eastward advection
1094 favours the MAW entrance in the Sicily Channel, allowing cool and nutrient enriched waters to enter
1095 the Channel. This resulted in an increased planktonic foraminifera flux and a higher presence of *G.*
1096 *inflata*, *G. truncatulinoides* or *G. bulloides*, which are taxa associated with the western basin. On the
1097 other hand, during summer, the eastward advection is reduced and the LIW dominates the water
1098 column, favorizing the increase of species associated with the eastern basin, such as *G. ruber*, and
1099 *G. ruber* (pink). Our correlation data with both SST and chlorophyll-*a* showed that *G. inflata* was
1100 associated with cool and nutrient rich waters. In contrast, both *G. ruber* species were associated
1101 with warm and oligotrophic waters, which agrees with their ecology. Surprisingly, no significant
1102 trends were identified for either *G. truncatulinoides* or *G. bulloides*. As *G. bulloides* flux increased
1103 coincidently with the benthic foraminifera one, we considered that this species might have a
1104 resuspended origin. The comparison with integrated annual data from other sediment trap
1105 experiments conducted in in different regions of the Mediterranean basin, our fluxes and diversity
1106 data indicated that the Sicily Channel can be considered a transitional zone in regard to planktonic
1107 foraminifera populations: annualized fluxes were lower compared to the westernmost Alboran Sea,
1108 but higher than in the easternmost Levantine basin. However, the Sicily Channel exhibited the
1109 highest diversity values across all the sites analyzed, highlighting the influence of both the western
1110 and eastern basins. Finally, the planktonic foraminifera assemblages from the sediment trap were

also compared with seabed sediment assemblages. Overall, both eutrophic and oligotrophic taxa were more abundant in the seabed sediment, however, *G. inflata* dominated the assemblages in the closest samples to the sediment trap location. Our dataset was similar to the assemblages from sites 342 and 407 (Incarbona et al., 2019) but different than the ones from the MARGO core-tops. This is likely due to the fact that they represented different time periods. Finally, the high-resolution chronology from sites 342 and 407 allowed to show that the planktonic foraminifera population shift likely developed during the late Holocene prior to the industrial period. However, the causes of this shift remain uncertain, and our results call for increasing the monitoring of planktonic foraminifera populations and accentuating the comparisons between recent and seabed sediment assemblages in the Mediterranean to determine if the trends suggested by our data are the result of the recent environmental change.

Data availability. All data used in this study are presented in the Supplement and are available online at doi: 10.17632/tp4v6hm7dc.1 (Béjard et al., 2023).

Supplement. The supplement related to this article is available online at:

Author contributions. ASRH, FJS and TMB designed the study. JPT designed Fig. 1 and contributed to planktonic foraminifera identification and imaging. ASV and ILC provided the JERICO C01 sediment trap samples and led the sample processing. TMB led the microscopy and image analysis, the foraminifera study, statistical analysis and wrote the manuscript with feedback from all authors.

Competing interests. The contact author has declared that none of the authors has any competing interests.

Acknowledgements. The authors would like to thank Aidan Hunter from the BAS (Cambridge) for the statistical analysis inputs and Francesca Bulian (University of Groningen) for benthic foraminifera identification support.

Financial support. This research has been supported by the Ministerio de Ciencia e Innovación (grant nos. RTI2018-099489-B-100, PID2021-128322NB-100, and PRE2019-089091). This research has also received funding from the JERICO project under the FP7 contract agreement nº 262584 and supported by ISMAR, CNR. ASV acknowledges the financial support by the Catalan Government Grups de Recerca Consolidats grant (2021 SGR 01195). This project has received funding from the project BASELINE (grant no. PID2021- 126495NB-741 C33) granted by the Spanish Ministry of Science and Innovation and Universities (Andrés S. Rigual-Hernández).

References

Aldridge, D., Beer, C. J., and Purdie, D. A.: Calcification in the planktonic foraminifera *Globigerina bulloides*; linked to phosphate concentrations in surface waters of the North Atlantic Ocean, Biogeosciences, 9, 1725–1739, https://doi.org/10.5194/bg-9-1725-2012, 2012.

Álvarez, M., Sanleón-Bartolomé, H., Tanhua, T., Mintrop, L., Luchetta, A., Cantoni, C., Schroeder, K., and Civitarese, G.: The CO_2 system in the Mediterranean Sea: a basin wide perspective, Ocean Sci., 10, 69–92, https://doi.org/10.5194/os-10-69-2014, 2014.

Astraldi, M., Gasparini, G. P., Gervasio, L., and Salusti, E.: Dense Water Dynamics along the Channel of Sicily (Mediterranean Sea), J. Phys. Oceanogr., 31, 3457–3475, https://doi.org/10.1175/1520-0485(2001)031<3457:DWDATS>2.0.CO;2, 2001.

Astraldi, M., Gasparini, G. P., Vetrano, A., and Vignudelli, S.: Hydrographic characteristics and interannual variability of water masses in the central Mediterranean: a sensitivity test for long-term changes in the Mediterranean Sea, Deep Sea Research Part I: Oceanographic Research Papers, 49, 661–680, https://doi.org/10.1016/S0967-0637(01)00059-0, 2002.

Avnaim-Katav, S., Herut, B., Rahav, E., Katz, T., Weinstein, Y., Alkalay, R., Berman-Frank, I., Zlatkin, O., and Almogi-Labin, A.: Sediment trap and deep sea coretop sediments as tracers of recent changes in planktonic foraminifera assemblages in the southeastern ultra-oligotrophic Levantine Basin, Deep Sea Research Part II: Topical Studies in Oceanography, 171, 104669, https://doi.org/10.1016/j.dsr2.2019.104669, 2020.

Azibeiro, L. A., Kučera, M., Jonkers, L., Cloke-Hayes, A., and Sierro, F. J.: Nutrients and hydrography explain the composition of recent Mediterranean planktonic foraminiferal assemblages, Marine Micropaleontology, 179, 102201, https://doi.org/10.1016/j.marmicro.2022.102201, 2023.

Balestra, B., Grunert, P., Ausin, B., Hodell, D., Flores, J.-A., Alvarez-Zarikian, C. A., Hernandez-Molina, F. J., Stow, D., Piller, W. E., and Paytan, A.: Coccolithophore and benthic foraminifera distribution patterns in the Gulf of Cadiz and Western Iberian Margin during Integrated Ocean Drilling Program (IODP) Expedition 339, Journal of Marine Systems, 170, 50–67, https://doi.org/10.1016/j.jmarsys.2017.01.005, 2017.

Bárcena, M. A., Flores, J. A., Sierro, F. J., Pérez-Folgado, M., Fabres, J., Calafat, A., and Canals, M.: Planktonic response to main oceanographic changes in the Alboran Sea (Western Mediterranean) as documented in sediment traps and surface sediments, Marine Micropaleontology, 53, 423–445, https://doi.org/10.1016/j.marmicro.2004.09.009, 2004.

Barker, S. and Elderfield, H.: Foraminiferal Calcification Response to Glacial-Interglacial Changes in Atmospheric CO_2, Science, 297, 833–836, https://doi.org/10.1126/science.1072815, 2002.

Bé, A. W. H., Hutson, W. H., and Be, A. W. H.: Ecology of Planktonic Foraminifera and Biogeographic Patterns of Life and Fossil Assemblages in the Indian Ocean, Micropaleontology, 23, 369, https://doi.org/10.2307/1485406, 1977.

Beer, C. J., Schiebel, R., and Wilson, P. A.: Testing planktonic foraminiferal shell weight as a surface water [CO_3^{2-}] proxy using plankton net samples, Geology, 38, 103–106, https://doi.org/10.1130/G30150.1, 2010.

Béjard, T. M., Rigual-Hernández, A. S., Flores, J. A., Tarruella, J. P., Durrieu De Madron, X., Cacho, I., Haghipour, N., Hunter, A., and Sierro, F. J.: Calcification response of planktonic foraminifera to environmental change in the western Mediterranean Sea during the industrial era, Biogeosciences, 20, 1505–1528, https://doi.org/10.5194/bg-20-1505-2023, 2023.

Béranger, K., Mortier, L., Gasparini, G.-P., Gervasio, L., Astraldi, M., and Crépon, M.: The dynamics of the Sicily Channel: a comprehensive study from observations and models, Deep Sea Research Part II: Topical Studies in Oceanography, 51, 411–440, https://doi.org/10.1016/j.dsr2.2003.08.004, 2004.

Bergamasco, A. and Malanotte-Rizzoli, P.: The circulation of the Mediterranean Sea: a historical review of experimental investigations, Advances in Oceanography and Limnology, 1, 11–28, https://doi.org/10.1080/19475721.2010.491656, 2010.

Bethoux, J. P., Gentili, B., Morin, P., Nicolas, E., Pierre, C., and Ruiz-Pino, D.: The Mediterranean Sea: a miniature ocean for climatic and environmental studies and a key for the climatic functioning of the North Atlantic, Progress in Oceanography, 44, 131–146, https://doi.org/10.1016/S0079-6611(99)00023-3, 1999.

Bijma, J., Faber, W. W., and Hemleben, C.: Temperature and salinity limits for growth and survival of some planktonic foraminifers in laboratory cultures, The Journal of Foraminiferal Research, 20, 95–116, https://doi.org/10.2113/gsjfr.20.2.95, 1990.

Bijma, J., Hönisch, B., and Zeebe, R. E.: Impact of the ocean carbonate chemistry on living foraminiferal shell weight: Comment on "Carbonate ion concentration in glacial-age deep waters of the Caribbean Sea" by W. S. Broecker and E. Clark: COMMENT, Geochem.-Geophys.-Geosyst., 3, 1–7, https://doi.org/10.1029/2002GC000388, 2002.

Bouzinac, C., Font, J., and Millot, C.: Hydrology and currents observed in the channel of Sardinia during the PRIMO-1 experiment from November 1993 to October 1994, Journal of Marine Systems, 20, 333–355, https://doi.org/10.1016/S0924-7963(98)00074-8, 1999.

Chapman, M. R.: Seasonal production patterns of planktonic foraminifera in the NE Atlantic Ocean: Implications for paleotemperature and hydrographic reconstructions: CURRENTS, Paleoceanography, 25, https://doi.org/10.1029/2008PA001708, 2010.

Chernihovsky, N., Torfstein, A., and Almogi-Labin, A.: Seasonal flux patterns of planktonic foraminifera in a deep, oligotrophic, marginal sea: Sediment trap time series from the Gulf of Aqaba, northern Red Sea, Deep Sea Research Part I: Oceanographic Research Papers, 140, 78–94, https://doi.org/10.1016/j.dsr.2018.08.003, 2018.

Chernihovsky, N., Torfstein, A., and Almogi-Labin, A.: Daily timescale dynamics of planktonic foraminifera shell-size distributions, Front. Mar. Sci., 10, 1126398, https://doi.org/10.3389/fmars.2023.1126398, 2023.

Cisneros, M., Cacho, I., Frigola, J., Canals, M., Masqué, P., Martrat, B., Casado, M., Grimalt, J. O., Pena, L. D., Margaritelli, G., and Lirer, F.: Sea surface temperature variability in the central-western Mediterranean Sea during the last 2700 years: a multi-proxy and multi-record approach, Clim. Past, 12, 849–869, https://doi.org/10.5194/cp-12-849-2016, 2016.

Dittert, N., Baumann, K.-H., Bickert, T., Henrich, R., Huber, R., Kinkel, H., and Meggers, H.: Carbonate Dissolution in the Deep-Sea: Methods, Quantification and Paleoceanographic Application, in: Use of Proxies in Paleoceanography, edited by: Fischer, G. and Wefer, G., Springer Berlin Heidelberg, Berlin, Heidelberg, 255–284, https://doi.org/10.1007/978-3-642-58646-0_10, 1999.

D'Ortenzio, F.: On the trophic regimes of the Mediterranean Sea: a satellite analysis, 2009.

Ducassou, E., Hassan, R., Gonthier, E., Duprat, J., Hanquiez, V., and Mulder, T.: Biostratigraphy of the last 50 kyr in the contourite depositional system of the Gulf of Cádiz, Marine Geology, 395, 285–300, https://doi.org/10.1016/j.margeo.2017.09.014, 2018.

Durrieu de Madron, X., Houpert, L., Puig, P., Sanchez-Vidal, A., Testor, P., Bosse, A., Estournel, C., Somot, S., Bourrin, F., Bouin, M. N., Beauverger, M., Beguery, L., Calafat, A., Canals, M., Cassou, C., Coppola, L., Dausse, D., D'Ortenzio, F., Font, J., Heussner, S., Kunesch, S., Lefevre, D., Le Goff, H., Martín, J., Mortier, L., Palanques, A., and Raimbault, P.: Interaction of dense shelf water cascading and open-sea convection in the northwestern Mediterranean during winter 2012: SHELF CASCADING AND OPEN-SEA CONVECTION, Geophys. Res. Lett., 40, 1379–1385, https://doi.org/10.1002/grl.50331, 2013.

Fox, L., Stukins, S., Hill, T., and Miller, C. G.: Quantifying the Effect of Anthropogenic Climate Change on Calcifying Plankton, Sci Rep, 10, 1620, https://doi.org/10.1038/s41598-020-58501-w, 2020.

Garcia-Solsona, E., Pena, L. D., Paredes, E., Pérez-Asensio, J. N., Quirós-Collazos, L., Lirer, F., and Cacho, I.: Rare earth elements and Nd isotopes as tracers of modern ocean circulation in the central Mediterranean Sea, Progress in Oceanography, 185, 102340, https://doi.org/10.1016/j.pocean.2020.102340, 2020.

Gasparini, G. P., Smeed, D. A., Alderson, S., Sparnocchia, S., Vetrano, A., and Mazzola, S.: Tidal and subtidal currents in the Strait of Sicily, J. Geophys. Res., 109, 2003JC002011, https://doi.org/10.1029/2003JC002011, 2004.

Gasparini, G. P., Ortona, A., Budillon, G., Astraldi, M., and Sansone, E.: The effect of the Eastern Mediterranean Transient on the hydrographic characteristics in the Channel of Sicily and in the Tyrrhenian Sea, Deep Sea Research Part I: Oceanographic Research Papers, 52, 915–935, https://doi.org/10.1016/j.dsr.2005.01.001, 2005.

Gaudy, R., Youssara, F., Diaz, F., and Raimbault, P.: Biomass, metabolism and nutrition of zooplankton in the Gulf of Lions (NW Mediterranean), Oceanologica Acta, 26, 357–372, https://doi.org/10.1016/S0399-1784(03)00016-1, 2003.

Grifoll, M., Cerralbo, P., Guillén, J., Espino, M., Hansen, L. B., and Sánchez-Arcilla, A.: Characterization of bottom sediment resuspension events observed in a micro-tidal bay, Ocean Sci., 15, 307–319, https://doi.org/10.5194/os-15-307-2019, 2019.

Hassoun, A. E. R., Gemayel, E., Krasakopoulou, E., Goyet, C., Abboud-Abi Saab, M., Guglielmi, V., Touratier, F., and Falco, C.: Acidification of the Mediterranean Sea from anthropogenic carbon penetration, Deep Sea Research Part I: Oceanographic Research Papers, 102, 1–15, https://doi.org/10.1016/j.dsr.2015.04.005, 2015.

Hassoun, A. E. R., Bantelman, A., Canu, D., Comeau, S., Galdies, C., Gattuso, J.-P., Giani, M., Grelaud, M., Hendriks, I. E., Ibello, V., Idrissi, M., Krasakopoulou, E., Shaltout, N., Solidoro, C., Swarzenski, P. W., and Ziveri, P.: Ocean

1257 acidification research in the Mediterranean Sea: Status, trends and next steps, Front. Mar. Sci., 9, 892670,
1258 https://doi.org/10.3389/fmars.2022.892670, 2022.

1259 Hayes, A., Kucera, M., Kallel, N., Sbaffi, L., and Rohling, E. J.: Compilation of planktonic foraminifera modern data
1260 from the Mediterranean Sea, https://doi.org/10.1594/PANGAEA.227305, 2005.

1261 Hazan, O., Silverman, J., Sisma-Ventura, G., Ozer, T., Gertman, I., Shoham-Frider, E., Kress, N., and Rahav, E.:
1262 Mesopelagic Prokaryotes Alter Surface Phytoplankton Production during Simulated Deep Mixing Experiments
1263 in Eastern Mediterranean Sea Waters, Front. Mar. Sci., 5, 1, https://doi.org/10.3389/fmars.2018.00001, 2018.

1264 Hemleben, C., Spindler, M., and Anderson, O. R.: Modern Planktonic Foraminifera, 1989.

1265 Hernández-Almeida, I., Bárcena, M. A., Flores, J. A., Sierro, F. J., Sanchez-Vidal, A., and Calafat, A.: Microplankton
1266 response to environmental conditions in the Alboran Sea (Western Mediterranean): One year sediment trap
1267 record, Marine Micropaleontology, 78, 14–24, https://doi.org/10.1016/j.marmicro.2010.09.005, 2011.

1268 Heussner, S., Ratti, C., and Carbonne, J.: The PPS 3 time-series sediment trap and the trap sample processing
1269 techniques used during the ECOMARGE experiment, Continental Shelf Research, 10, 943–958,
1270 https://doi.org/10.1016/0278-4343(90)90069-X, 1990.

1271 Heussner, S., Durrieu de Madron, X., Calafat, A., Canals, M., Carbonne, J., Delsaut, N., and Saragoni, G.: Spatial and
1272 temporal variability of downward particle fluxes on a continental slope: Lessons from an 8-yr experiment in
1273 the Gulf of Lions (NW Mediterranean), Marine Geology, 234, 63–92,
1274 https://doi.org/10.1016/j.margeo.2006.09.003, 2006.

1275 Houpert, L., Durrieu de Madron, X., Testor, P., Bosse, A., D'Ortenzio, F., Bouin, M. N., Dausse, D., Le Goff, H.,
1276 Kunesch, S., Labaste, M., Coppola, L., Mortier, L., and Raimbault, P.: Observations of open-ocean deep
1277 convection in the northwestern Mediterranean Sea: Seasonal and interannual variability of mixing and deep
1278 water masses for the 2007-2013 Period: DEEP CONVECTION OBS. NWMED 2007-2013, J. Geophys. Res.
1279 Oceans, 121, 8139–8171, https://doi.org/10.1002/2016JC011857, 2016.

1280 Huertas, I. E., Ríos, A. F., García-Lafuente, J., Navarro, G., Makaoui, A., Sánchez-Román, A., Rodriguez-Galvez, S.,
1281 Orbi, A., Ruíz, J., and Pérez, F. F.: Atlantic forcing of the Mediterranean oligotrophy: ATLANTIC FORCING OF
1282 MEDITERRANEAN OLIGOTROPHY, Global Biogeochem. Cycles, 26, n/a-n/a,
1283 https://doi.org/10.1029/2011GB004167, 2012.

1284 Incarbona, A., Jonkers, L., Ferraro, S., Sprovieri, R., and Tranchida, G.: Sea Surface Temperatures and
1285 Paleoenvironmental Variability in the Central Mediterranean During Historical Times Reconstructed Using
1286 Planktonic Foraminifera, Paleoceanog and Paleoclimatol, 34, 394–408,
1287 https://doi.org/10.1029/2018PA003529, 2019.

1288

1289 Incarbona, A., Sprovieri, M., Lirer, F., and Sprovieri, R.: Surface and deep water conditions in the Sicily channel
1290 (central Mediterranean) at the time of sapropel S5 deposition, Palaeogeography, Palaeoclimatology,
1291 Palaeoecology, 306, 243–248, https://doi.org/10.1016/j.palaeo.2011.04.030, 2011.

1292 Jonkers, L. and Kučera, M.: Global analysis of seasonality in the shell flux of extant planktonic Foraminifera,
1293 Biogeosciences, 12, 2207–2226, https://doi.org/10.5194/bg-12-2207-2015, 2015.

1294 Jonkers, L., Hillebrand, H., and Kucera, M.: Global change drives modern plankton communities away from the pre-
1295 industrial state, Nature, 570, 372–375, https://doi.org/10.1038/s41586-019-1230-3, 2019.

1296 Jouini, M., Béranger, K., Arsouze, T., Beuvier, J., Thiria, S., Crépon, M., and Taupier-Letage, I.: The Sicily Channel
1297 surface circulation revisited using a neural clustering analysis of a high-resolution simulation, JGR Oceans, 121,
1298 4545–4567, https://doi.org/10.1002/2015JC011472, 2016.

1299 Kemle-von Mücke, S. and Oberhänsli, H.: The Distribution of Living Planktonic Foraminifera in Relation to Southeast
1300 Atlantic Oceanography, in: Use of Proxies in Paleoceanography, edited by: Fischer, G. and Wefer, G., Springer
1301 Berlin Heidelberg, Berlin, Heidelberg, 91–115, https://doi.org/10.1007/978-3-642-58646-0_3, 1999.

1302 Kiss, P., Jonkers, L., Hudáčková, N., Reuter, R. T., Donner, B., Fischer, G., and Kucera, M.: Determinants of Planktonic
1303 Foraminifera Calcite Flux: Implications for the Prediction of Intra- and Inter-Annual Pelagic Carbonate Budgets,
1304 Global Biogeochem Cycles, 35, https://doi.org/10.1029/2020GB006748, 2021.

1305 Kroeker, K. J., Kordas, R. L., Crim, R., Hendriks, I. E., Ramajo, L., Singh, G. S., Duarte, C. M., and Gattuso, J.: Impacts
1306 of ocean acidification on marine organisms: quantifying sensitivities and interaction with warming, Glob
1307 Change Biol, 19, 1884–1896, https://doi.org/10.1111/gcb.12179, 2013.

1308 Krom, M. D., Kress, N., Brenner, S., and Gordon, L. I.: Phosphorus limitation of primary productivity in the eastern
1309 Mediterranean Sea, Limnol. Oceanogr., 36, 424–432, https://doi.org/10.4319/lo.1991.36.3.0424, 1991.

1310 Krom, M. D., Woodward, E. M. S., Herut, B., Kress, N., Carbo, P., Mantoura, R. F. C., Spyres, G., Thingstad, T. F.,
1311 Wassmann, P., Wexels-Riser, C., Kitidis, V., Law, C. S., and Zodiatis, G.: Nutrient cycling in the south east
1312 Levantine basin of the eastern Mediterranean: Results from a phosphorus starved system, Deep Sea Research
1313 Part II: Topical Studies in Oceanography, 52, 2879–2896, https://doi.org/10.1016/j.dsr2.2005.08.009, 2005.
1314 Kuroyanagi, A. and Kawahata, H.: Vertical distribution of living planktonic foraminifera in the seas around Japan,
1315 Marine Micropaleontology, 53, 173–196, https://doi.org/10.1016/j.marmicro.2004.06.001, 2004.
1316 Lazzari, P., Mattia, G., Solidoro, C., Salon, S., Crise, A., Zavatarelli, M., Oddo, P., and Vichi, M.: The impacts of climate
1317 change and environmental management policies on the trophic regimes in the Mediterranean Sea: Scenario
1318 analyses, Journal of Marine Systems, 135, 137–149, https://doi.org/10.1016/j.jmarsys.2013.06.005, 2014.
1319 Lermusiaux, P. F. J. and Robinson, A. R.: Features of dominant mesoscale variability, circulation patterns and
1320 dynamics in the Channel of Sicily, Deep Sea Research Part I: Oceanographic Research Papers, 48, 1953–1997,
1321 https://doi.org/10.1016/S0967-0637(00)00114-X, 2001.
1322 Lirer, F., Sprovieri, M., Vallefuoco, M., Ferraro, L., Pelosi, N., Giordano, L., and Capotondi, L.: Planktonic
1323 foraminifera as bio-indicators for monitoring the climatic changes that have occurred over the past 2000 years
1324 in the southeastern Tyrrhenian Sea, Integrative Zoology, 9, 542–554, https://doi.org/10.1111/1749-
1325 4877.12083, 2014.
1326 Lombard, F., Erez, J., Michel, E., and Labeyrie, L.: Temperature effect on respiration and photosynthesis of the
1327 symbiont-bearing planktonic foraminifera *Globigerinoides ruber* , *Orbulina universa* , and *Globigerinella*
1328 *siphonifera*, Limnol. Oceanogr., 54, 210–218, https://doi.org/10.4319/lo.2009.54.1.0210, 2009.
1329 Lombard, F., Labeyrie, L., Michel, E., Bopp, L., Cortijo, E., Retailleau, S., Howa, H., and Jorissen, F.: Modelling
1330 planktonic foraminifer growth and distribution using an ecophysiological multi-species approach,
1331 Biogeosciences, 8, 853–873, https://doi.org/10.5194/bg-8-853-2011, 2011.
1332 Macias, D., Cózar, A., Garcia-Gorriz, E., González-Fernández, D., and Stips, A.: Surface water circulation develops
1333 seasonally changing patterns of floating litter accumulation in the Mediterranean Sea. A modelling approach,
1334 Marine Pollution Bulletin, 149, 110619, https://doi.org/10.1016/j.marpolbul.2019.110619, 2019.
1335 Malanotte-Rizzoli, P., Artale, V., Borzelli-Eusebi, G. L., Brenner, S., Crise, A., Gacic, M., Kress, N., Marullo, S., Ribera
1336 d'Alcalà, M., Sofianos, S., Tanhua, T., Theocharis, A., Alvarez, M., Ashkenazy, Y., Bergamasco, A., Cardin, V.,
1337 Carniel, S., Civitarese, G., D'Ortenzio, F., Font, J., Garcia-Ladona, E., Garcia-Lafuente, J. M., Gogou, A., Gregoire,
1338 M., Hainbucher, D., Kontoyannis, H., Kovacevic, V., Kraskapoulou, E., Kroskos, G., Incarbona, A., Mazzocchi,
1339 M. G., Orlic, M., Ozsoy, E., Pascual, A., Poulain, P.-M., Roether, W., Rubino, A., Schroeder, K., Siokou-Frangou,
1340 J., Souvermezoglou, E., Sprovieri, M., Tintoré, J., and Triantafyllou, G.: Physical forcing and
1341 physical/biochemical variability of the Mediterranean Sea: a review of unresolved issues and directions for
1342 future research, Ocean Sci., 10, 281–322, https://doi.org/10.5194/os-10-281-2014, 2014.
1343 Mallo, M., Ziveri, P., Mortyn, P. G., Schiebel, R., and Grelaud, M.: Low planktonic foraminiferal diversity and
1344 abundance observed in a spring 2013 west–east Mediterranean Sea plankton tow transect, Biogeosciences,
1345 14, 2245–2266, https://doi.org/10.5194/bg-14-2245-2017, 2017.
1346 Margaritelli, G., Lirer, F., Schroeder, K., Alberico, I., Dentici, M. P., and Caruso, A.: Globorotalia truncatulinoides in
1347 Central - Western Mediterranean Sea during the Little Ice Age, Marine Micropaleontology, 161, 101921,
1348 https://doi.org/10.1016/j.marmicro.2020.101921, 2020.
1349 Margaritelli, G., Lirer, F., Schroeder, K., Cloke-Hayes, A., Caruso, A., Capotondi, L., Broggy, T., Cacho, I., and Sierro,
1350 F. J.: Globorotalia truncatulinoides in the Mediterranean Basin during the Middle–Late Holocene: Bio-
1351 Chronological and Oceanographic Indicator, Geosciences, 12, 244,
1352 https://doi.org/10.3390/geosciences12060244, 2022.
1353 Marshall, B. J., Thunell, R. C., Henehan, M. J., Astor, Y., and Wejnert, K. E.: Planktonic foraminiferal area density as
1354 a proxy for carbonate ion concentration: A calibration study using the Cariaco Basin ocean time series:
1355 FORAMINIFERAL AREA DENSITY [CO_3^{2-}] PROXY, Paleoceanography, 28, 363–376,
1356 https://doi.org/10.1002/palo.20034, 2013.
1357 Milker, Y. and Schmiedl, G.: A taxonomic guide to modern benthic shelf foraminifera of the western Mediterranean
1358 Sea, Palaeontologia Electronica, https://doi.org/10.26879/271, 2012.
1359 Millot, C.: Mesoscale and seasonal variabilities of the circulation in the western Mediterranean, Dynamics of
1360 Atmospheres and Oceans, 15, 179–214, https://doi.org/10.1016/0377-0265(91)90020-G, 1991.
1361 Millot, C.: Circulation in the Western Mediterranean Sea, Journal of Marine Systems, 20, 423–442,
1362 https://doi.org/10.1016/S0924-7963(98)00078-5, 1999.

Millot, C. and Taupier-Letage, I.: Circulation in the Mediterranean Sea, in: The Mediterranean Sea, vol. 5K, edited by: Saliot, A., Springer Berlin Heidelberg, Berlin, Heidelberg, 29–66, https://doi.org/10.1007/b107143, 2005.

de Moel, H., Ganssen, G. M., Peeters, F. J. C., Jung, S. J. A., Kroon, D., Brummer, G. J. A., and Zeebe, R. E.: Planktonic foraminiferal shell thinning in the Arabian Sea due to anthropogenic ocean acidification?, Biogeosciences, 6, 1917–1925, https://doi.org/10.5194/bg-6-1917-2009, 2009.

Morán, X. and Estrada, M.: Short-term variability of photosynthetic parameters and particulate and dissolved primary production in the Alboran Sea (SW Mediterranean), Mar. Ecol. Prog. Ser., 212, 53–67, https://doi.org/10.3354/meps212053, 2001.

Moy, A. D., Howard, W. R., Bray, S. G., and Trull, T. W.: Reduced calcification in modern Southern Ocean planktonic foraminifera, Nature Geosci, 2, 276–280, https://doi.org/10.1038/ngeo460, 2009.

Navarro, G., Almaraz, P., Caballero, I., Vázquez, Á., and Huertas, I. E.: Reproduction of Spatio-Temporal Patterns of Major Mediterranean Phytoplankton Groups from Remote Sensing OC-CCI Data, Front. Mar. Sci., 4, 246, https://doi.org/10.3389/fmars.2017.00246, 2017.

Nielsen, S. N.: Numerical Ecology. Legendre P. and Legendre L., second ed., Elsevier, Amsterdam, p. 853, 1998., Ecological Modelling, 132, 303–304, https://doi.org/10.1016/S0304-3800(00)00291-X, 2000.

Ortiz, J. D. and Mix, A. C.: Comparison of Imbrie-Kipp Transfer Function and modern analog temperature estimates using sediment trap and core top foraminiferal faunas, Paleoceanography, 12, 175–190, https://doi.org/10.1029/96PA02878, 1997.

Osborne, E. B., Thunell, R. C., Marshall, B. J., Holm, J. A., Tappa, E. J., Benitez-Nelson, C., Cai, W., and Chen, B.: Calcification of the planktonic foraminifera *Globigerina bulloides* and carbonate ion concentration: Results from the Santa Barbara Basin, Paleoceanography, 31, 1083–1102, https://doi.org/10.1002/2016PA002933, 2016.

Ozer, T., Gertman, I., Kress, N., Silverman, J., and Herut, B.: Interannual thermohaline (1979–2014) and nutrient (2002–2014) dynamics in the Levantine surface and intermediate water masses, SE Mediterranean Sea, Global and Planetary Change, 151, 60–67, https://doi.org/10.1016/j.gloplacha.2016.04.001, 2017.

Pallacks, S., Ziveri, P., Schiebel, R., Vonhof, H., Rae, J. W. B., Littley, E., Garcia-Orellana, J., Langer, G., Grelaud, M., and Martrat, B.: Anthropogenic acidification of surface waters drives decreased biogenic calcification in the Mediterranean Sea, Commun Earth Environ, 4, 301, https://doi.org/10.1038/s43247-023-00947-7, 2023.

Pinardi, N., Zavatarelli, M., Adani, M., Coppini, G., Fratianni, C., Oddo, P., Simoncelli, S., Tonani, M., Lyubartsev, V., Dobricic, S., and Bonaduce, A.: Mediterranean Sea large-scale low-frequency ocean variability and water mass formation rates from 1987 to 2007: A retrospective analysis, Progress in Oceanography, 132, 318–332, https://doi.org/10.1016/j.pocean.2013.11.003, 2015.

Poore, R. Z., Tedesco, K. A., and Spear, J. W.: Seasonal Flux and Assemblage Composition of Planktonic Foraminifers from a Sediment-Trap Study in the Northern Gulf of Mexico, Journal of Coastal Research, 63, 6–19, https://doi.org/10.2112/SI63-002.1, 2013.

Prell, W. The Stability of Low-Latitude Sea-Surface Temperatures, an Evaluation of the CLIMAP Reconstruction with Emphasis on the Positive SST Anomalies. *Report No. TR025* (US Department of Energy), 1985.

Pujol, C. and Grazzini, C. V.: Distribution patterns of live planktonic foraminifers as related to regional hydrography and productive systems of the Mediterranean Sea, Marine Micropaleontology, 25, 187–217, https://doi.org/10.1016/0377-8398(95)00002-I, 1995.

Raimbault, P., Pouvesle, W., Diaz, F., Garcia, N., and Sempéré, R.: Wet-oxidation and automated colorimetry for simultaneous determination of organic carbon, nitrogen and phosphorus dissolved in seawater, Marine Chemistry, 66, 161–169, https://doi.org/10.1016/S0304-4203(99)00038-9, 1999.

Rebotim, A., Voelker, A. H. L., Jonkers, L., Waniek, J. J., Meggers, H., Schiebel, R., Fraile, I., Schulz, M., and Kucera, M.: Factors controlling the depth habitat of planktonic foraminifera in the subtropical eastern North Atlantic, Biogeosciences, 14, 827–859, https://doi.org/10.5194/bg-14-827-2017, 2017.

Retailleau, S., Schiebel, R., and Howa, H.: Population dynamics of living planktonic foraminifers in the hemipelagic southeastern Bay of Biscay, Marine Micropaleontology, 80, 89–100, https://doi.org/10.1016/j.marmicro.2011.06.003, 2011.

Rigual-Hernández, A. S., Sierro, F. J., Bárcena, M. A., Flores, J. A., and Heussner, S.: Seasonal and interannual changes of planktonic foraminiferal fluxes in the Gulf of Lions (NW Mediterranean) and their implications for paleoceanographic studies: Two 12-year sediment trap records, Deep Sea Research Part I: Oceanographic Research Papers, 66, 26–40, https://doi.org/10.1016/j.dsr.2012.03.011, 2012.

Robinson, A. R. and Golnaraghi, M.: The Physical and Dynamical Oceanography of the Mediterranean Sea, in: Ocean Processes in Climate Dynamics: Global and Mediterranean Examples, edited by: Malanotte-Rizzoli, P. and Robinson, A. R., Springer Netherlands, Dordrecht, 255–306, https://doi.org/10.1007/978-94-011-0870-6_12, 1994.

Robinson, A. R., Sellschopp, J., Warn-Varnas, A., Leslie, W. G., Lozano, C. J., Haley Jr, P. J., Anderson, L. A., and Lermusiaux, P. F. J.: The Atlantic Ionian Stream, Journal of Marine Systems, 129–156, 1999.

Romero, O., Boeckel, B., Donner, B., Lavik, G., Fischer, G., and Wefer, G.: Seasonal productivity dynamics in the pelagic central Benguela System inferred from the flux of carbonate and silicate organisms, Journal of Marine Systems, 37, 259–278, https://doi.org/10.1016/S0924-7963(02)00189-6, 2002.

Salmon, K. H., Anand, P., Sexton, P. F., and Conte, M.: Upper ocean mixing controls the seasonality of planktonic foraminifer fluxes and associated strength of the carbonate pump in the oligotrophic North Atlantic, Biogeosciences, 12, 223–235, https://doi.org/10.5194/bg-12-223-2015, 2015.

Schiebel, R.: Planktonic foraminiferal sedimentation and the marine calcite budget: MARINE CALCITE BUDGET, Global Biogeochem. Cycles, 16, 3-1-3–21, https://doi.org/10.1029/2001GB001459, 2002.

Schiebel, R. and Hemleben, C.: Modern planktonic foraminifera, Paläontol. Z., 79, 135–148, https://doi.org/10.1007/BF03021758, 2005.

Schiebel, R. and Hemleben, C.: Planktonic Foraminifers in the Modern Ocean, Springer Berlin Heidelberg, Berlin, Heidelberg, https://doi.org/10.1007/978-3-662-50297-6, 2017.

Schiebel, R., Waniek, J., Bork, M., and Hemleben, C.: Planktonic foraminiferal production stimulated by chlorophyll redistribution and entrainment of nutrients, Deep Sea Research Part I: Oceanographic Research Papers, 48, 721–740, https://doi.org/10.1016/S0967-0637(00)00065-0, 2001.

Schiebel, R., Zeltner, A., Treppke, U. F., Waniek, J. J., Bollmann, J., Rixen, T., and Hemleben, C.: Distribution of diatoms, coccolithophores and planktonic foraminifers along a trophic gradient during SW monsoon in the Arabian Sea, Marine Micropaleontology, 51, 345–371, https://doi.org/10.1016/j.marmicro.2004.02.001, 2004.

Schmidt, D. N., Lazarus, D., Young, J. R., and Kucera, M.: Biogeography and evolution of body size in marine plankton, Earth-Science Reviews, 78, 239–266, https://doi.org/10.1016/j.earscirev.2006.05.004, 2006.

Schroeder, K., Chiggiato, J., Josey, S. A., Borghini, M., Aracri, S., and Sparnocchia, S.: Rapid response to climate change in a marginal sea, Sci Rep, 7, 4065, https://doi.org/10.1038/s41598-017-04455-5, 2017.

Schroeder, K., Gasparini, G. P., Borghini, M., Cerrati, G., and Delfanti, R.: Biogeochemical tracers and fluxes in the Western Mediterranean Sea, spring 2005, Journal of Marine Systems, 80, 8–24, https://doi.org/10.1016/j.jmarsys.2009.08.002, 2010.

Sen Gupta, B. K. (Ed.): Modern foraminifera, first published in paperback., Kluwer, Dordrecht, 371 pp., 2002.

Siccha, M. and Kucera, M.: ForCenS, a curated database of planktonic foraminifera census counts in marine surface sediment samples, Sci Data, 4, 170109, https://doi.org/10.1038/sdata.2017.109, 2017.

Siokou-Frangou, I., Christaki, U., Mazzocchi, M. G., Montresor, M., Ribera d'Alcalá, M., Vaqué, D., and Zingone, A.: Plankton in the open Mediterranean Sea: a review, Biogeosciences, 7, 1543–1586, https://doi.org/10.5194/bg-7-1543-2010, 2010.

Skinner, L. C. and McCave, I. N.: Analysis and modelling of gravity- and piston coring based on soil mechanics, Marine Geology, 199, 181–204, https://doi.org/10.1016/S0025-3227(03)00127-0, 2003.

Takagi, H., Kimoto, K., Fujiki, T., Saito, H., Schmidt, C., Kucera, M., and Moriya, K.: Characterizing photosymbiosis in modern planktonic foraminifera, Biogeosciences, 16, 3377–3396, https://doi.org/10.5194/bg-16-3377-2019, 2019.

Takahashi, K. and Be, A. W. H.: Planktonic foraminifera: factors controlling sinking speeds, Deep Sea Research Part A. Oceanographic Research Papers, 31, 1477–1500, https://doi.org/10.1016/0198-0149(84)90083-9, 1984.

Toucanne, S., Mulder, T., Schönfeld, J., Hanquiez, V., Gonthier, E., Duprat, J., Cremer, M., and Zaragosi, S.: Contourites of the Gulf of Cadiz: A high-resolution record of the paleocirculation of the Mediterranean outflow water during the last 50,000 years, Palaeogeography, Palaeoclimatology, Palaeoecology, 246, 354–366, https://doi.org/10.1016/j.palaeo.2006.10.007, 2007.

Warn-Varnas, A., Sellschopp, J., Haley, P. J., Leslie, W. G., and Lozano, C. J.: Channel of Sicily water masses, Dynamics of Atmospheres and Oceans, 29, 437–469, https://doi.org/10.1016/S0377-0265(99)00014-7, 1999.

1467 Wilke, I., Meggers, H., and Bickert, T.: Depth habitats and seasonal distributions of recent planktonic foraminifers
1468   in the Canary Islands region (29°N) based on oxygen isotopes, Deep Sea Research Part I: Oceanographic
1469   Research Papers, 56, 89–106, https://doi.org/10.1016/j.dsr.2008.08.001, 2009.
1470 Wu, H., Liu, N., Peng, J., Ge, Y., and Kong, B.: Analysis and modelling on coring process of deep-sea gravity piston
1471   corer, J. eng., 2020, 900–905, https://doi.org/10.1049/joe.2020.0077, 2020.
1472 Wolfteich, C. M.: Sattelite-derived sea surface temperature, mesoscale variability, and foraminiferal production in
1473   the North Atlantic, M.Sc., MIT and WHOI, Cambridge, MS, 91 pp., 1994.
1474 Zarkogiannis, S. D., Iwasaki, S., Rae, J. W. B., Schmidt, M. W., Mortyn, P. G., Kontakiotis, G., Hertzberg, J. E., and
1475   Rickaby, R. E. M.: Calcification, Dissolution and Test Properties of Modern Planktonic Foraminifera From the
1476   Central Atlantic Ocean, Front. Mar. Sci., 9, 864801, https://doi.org/10.3389/fmars.2022.864801, 2022.

1477
1478
1479
1480
1481